Murujuga Rock Art Monitoring Program: Interim Environmental Quality Criteria Update 2025

Prepared for the Murujuga Aboriginal Corporation and the Department of Water and Environmental Regulation.

Prepared by: Nicola Armstrong, Katelyn Boase, Arne Bredin, Eddie Campbell, Noel Cressie, Thomas Di Loreto, Katy Evans, Ronald Fellows-Smith, Kliti Grice, Monica Gumulya, Toni Hannelly, Stephanie Hogg, Katherine Landwehr, David Lynch, Alex Martin, Ryan Mead-Hunter, Abraj Mohomed, Benjamin Mullins, Rebecca O'Leary, Anuradha Patel, Will Rickard, Sebastian Stanley.

Doc No	Current Rev	Revision Date	Checked By	Approved By
COPP21065-REP-G-110	1	29/05/2026	B. Mullins 	N. Armstrong 

Revision history

Revision No	Date	Revision Reason
A	01/09/2025	Preliminary for internal review
B	15/09/2025	Issued to DWER for peer review
C	02/02/2026	Updated following peer review
0	23/04/2026	Issued for use following close-out review
1	29/05/2026	Reissued for use following correction of minor technical errors in appendices

The data associated with this report is available on request from the Department of Water and Environmental Regulation.

Contents

List of Figures

List of Tables

1 Overview

1.1 Introduction

The Murujuga Rock Art Monitoring Program (**MRAMP**, the Program) is the most extensive scientific study to date to examine the impact of industrial air emissions on the rock art engravings of Murujuga, an area covering the Burrup Peninsula and Dampier Archipelago in Western Australia. The Program is overseen by the Department of Water and Environmental Regulation (**DWER**) in partnership with the Murujuga Aboriginal Corporation (**MAC**) and is a key component of the State Government's Murujuga Rock Art Strategy (**MRAS**, DWER, 2019b).

The Program incorporates extensive field measurements and laboratory (chamber) accelerated weathering studies on the five lithologies/rock types (granophyre, gabbro, granite, dolerite, basalt) which comprise the majority of petroglyph substrates. It consists of a detailed study design phase, followed by three to four years of detailed scientific studies, transitioning into ongoing monitoring and assessment against the Environmental Quality Criteria (**EQC**) established through the studies.

The MRAMP was established to determine whether accelerated weathering of rock art due to anthropogenic activities is occurring and to identify conditions for their protection. Management of the rock art will be undertaken using an Environmental Quality Management Framework (**EQMF**) and conditions needed to protect the rock art will be stated as EQC.

EQC will be clear, measurable and auditable.

The MRAMP considers all potential atmospheric impacts on the geology/geochemistry, microbiome and visual appearance of the rock surface and rock art. These include anthropogenic and natural effects and sources. Previous research has focused on air emissions with a potential to form acidic or basic compounds which may react with the rock surface, principally nitrogen dioxide (NO_2), sulfur dioxide (SO_2), and ammonia (NH_3). These emissions have been considered in some detail, however all natural and anthropogenic air contaminants are the focus of the program. For example, natural and anthropogenic particulate matter (PM, dust/soot) is also abundant in the region. Components in environmental dust are an important building block in the formation of the rock surface patina, which has more complex biogeochemical interactions compared to single gas species, including with microbes which cement the minerals to the rock surface. These interactions remain an area of ongoing study, both for the overall research project and for EQC development.

Chamber studies in the Monitoring Studies Report 2024 (Curtin University, 2024b) focused on combustion emissions from various sources, and gaseous NH_3. EQC for NO_2 and SO_2 were set as linked EQC as individual responses could not be differentiated from the experiments completed at that time. For the Monitoring Studies Report 2025 (Curtin University, 2025), chamber studies progressed to predominantly single gas species exposure studies, in order to differentiate between the relative effects of NO_2 and SO_2 in particular. In this process, the weaker effect of individual gas exposure required some revisions to the chamber studies method in order to improve reproducibility. Other weathering literature was reviewed which reinforced the findings of the Monitoring Studies Report 2025 (Curtin University, 2025) chamber studies using the revised method.

In general, single gas exposure studies found weaker effects from individual gas species and little or no effect from NO_2 within the concentration range possible experimentally (which is expected to be far above realistic environmental concentrations). This led to a revision of the chamber study

protocol and extensive searches of other weathering literature. As a result, Interim EQC have been significantly revised since the previous Interim EQC (Curtin University, 2024a). The future progression to a combined “weatherability index” EQC is expected and is outlined here. However, Interim EQC for individual gas species published previously (Curtin University, 2024a) have been included for continuity. Results from both bushfire and “sooty” fuels such as heavy fuel oil (HFO) and diesel appear to elicit a stronger response, which may be due to components other than gases. This will also be investigated in future EQC development.

This document sets out the updated Interim EQC based on the data collection and analyses from the first three years of monitoring studies and laboratory investigations. It is intended to be read in conjunction with the *Murujuga Rock Art Strategy* (**MRAS**, DWER, 2019b), *Murujuga Rock Art Monitoring Program:* Conceptual Model (DWER, 2021), *Murujuga Rock Art Monitoring Program:* Data Collection and Analysis Plan (Curtin University, 2022) and Monitoring Studies Report 2025 (Curtin University, 2025), as well as relevant methodology statements.

The information contained in this document supersedes the Interim EQC published in the *Interim Environmental Quality Criteria 2025* (Curtin University, 2024a) released in April 2025.

A primary outcome of MRAMP will be one or more EQC which are designed to ensure environmental values and environmental quality objectives of the Murujuga Rock Art Strategy (DWER, 2019b) can be maintained. The final EQC may take the form of a single combined weatherability index which combines all relevant species.

The EQC will complete the EQMF, to ensure the long-term protection of the Murujuga rock art from undesirable anthropogenic effects (DWER, 2019a; DWER, 2019b). In addition, the Murujuga Cultural Landscape was inscribed as Australia’s 21st World Heritage area in July 2025, being the country’s second cultural landscape World Heritage area and its first indigenous-led nomination. Ongoing monitoring against the EQC determined by MRAMP will be an important control to support the Murujuga Cultural Landscape World Heritage management plan.

This report summarises the development of the Interim EQC to date, a method for monitoring and comparison with these Interim EQC, and further work required to finalise the EQC over the course of the MRAMP research.

1.2 EQC concept

Historically, EQC were developed in the marine science field and refer to benchmark levels that trigger management attention and action to protect ecosystem structure and function, serving as standards for assessing environmental quality and determining regulatory limitations on contaminants.

The EQMF model for MRAMP, shown in Figure 1 (DWER, 2019b) is intended to build on the EQC to develop a comprehensive management framework. The concept of the EQMF is intended to ensure that environmental values can be maintained and environmental quality objectives can be achieved (DWER, 2019a). This is achieved in part through the appropriate application of EQC. EQC are the scientifically based limits of ‘acceptable’ change. The criteria are the benchmarks against which environmental monitoring data are compared to determine the extent to which environmental quality objectives have been met, and if not met, whether a management response is required.

Criteria should be clear, readily measurable and auditable, and standardised approaches should be given for measuring indicators and for comparison of monitoring data against the criteria.

- **Standard** EQC levels, denoted by the threshold to the high (red) region on the risk scale in Figure 1, represent limits above which sufficient evidence exists that impacts are likely to occur, within appropriate levels of confidence.
- **Guideline** EQC levels are set lower using appropriate uncertainty factors to determine the minimum level where any possible effects could theoretically occur. These levels are denoted as the threshold from low (green) to the uncertain (amber) regions of risk in Figure 1.

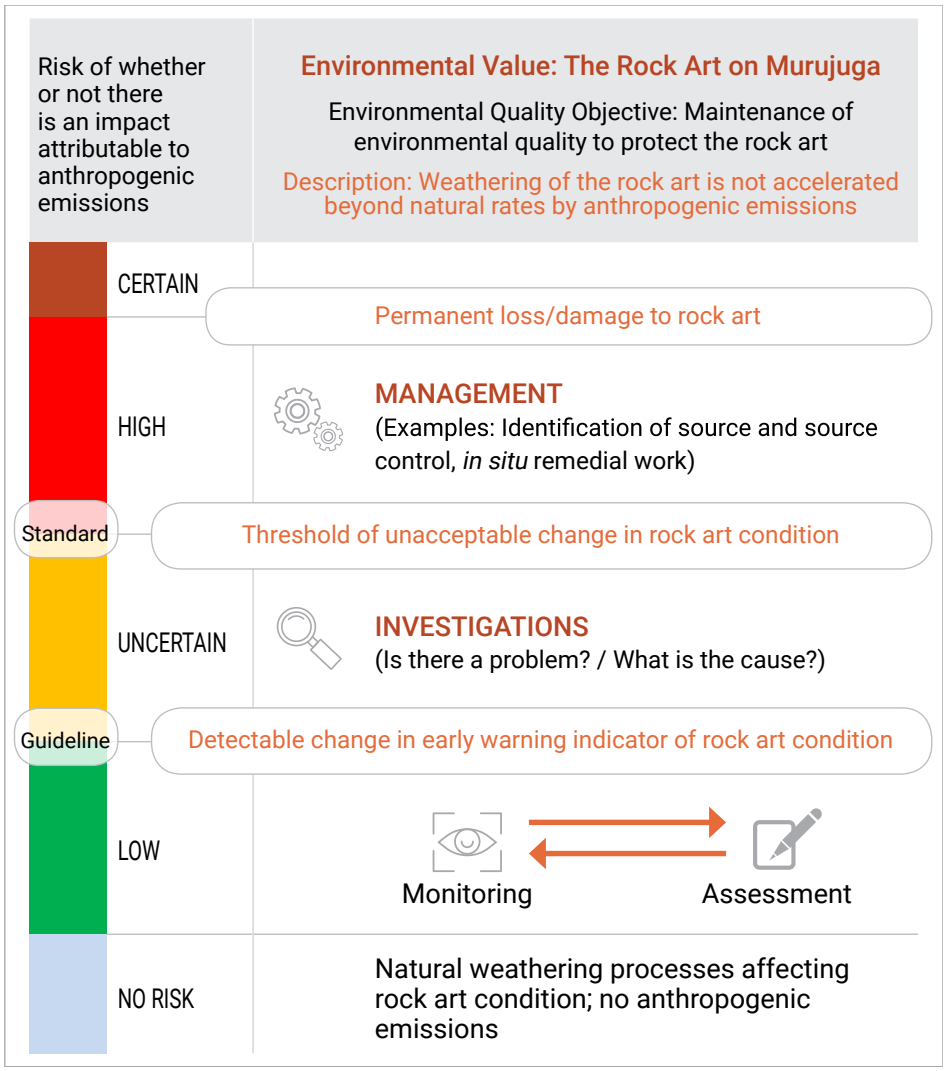

Figure 1: The Environmental Quality Management Framework for Murujuga, including Guideline and Standard EQC concepts (DWER 2019b).

EQC are generally developed based on the determination of nil or minimal effect levels or concentrations from environmental or experimental/clinical dose-response curves. Dose-response relationships have been used to establish thresholds for pollutant concentrations in other situations where rock-based heritage may be at risk from particular gases within the atmosphere (e.g., Bai and Yan, 2025; Broomandi et al., 2022; Visone et al., 2025).

A wide range of terminology is used to refer to the no-effect or minimal effect level in dose-response studies; in this document, the terms *No Observed Effect Concentration* (**NOEC**) or *Lowest Observed Effect Concentration* (**LOEC**) will be utilised for MRAMP, as they are the most widely used terminology in the field of ecotoxicology.

2 Methodology for EQC development

2.1 Summary of work to date

MRAMP includes a multi-year research program to determine appropriate EQC parameters. Three years of the planned studies (see Curtin University (2025)) are now complete. The work to date has established a mechanism by which accelerated weathering may occur, and has developed a sufficient dataset of laboratory testing to permit Interim EQC values to be established for NO_2, SO_2, and NH_3, as these are key primary gaseous pollutants emitted into the airshed.

Field observations of accelerated weathering in granophyre samples have been measured and can only be associated with anthropogenic activity (as opposed to natural causes). This weathering mechanism was replicated in the laboratory in the Monitoring Studies Report 2024 (Curtin University, 2024b) studies after multiple exposures to high levels of combustion gases and aerosols.

In the Monitoring Studies Report 2024 (Curtin University, 2024b), spatial relationships between rock surface porosity and NO_2 were presented and a guideline EQC was derived. However, subsequent chamber studies using NO_2 as a single gas species and literature searches have both revealed much weaker effects from NO_2 than previously suggested by MRAMP and other research (Neumann, 2025). Stronger effects have been found for SO_2 and NH_3. Based on historic emissions/exposure estimates and thermodynamic modelling, it is likely that synergistic effects between multiple pollutants and/or the rock surface microbiome may be required before weathering is accelerated.

Separate research Neumann (2025) has found accelerated weathering at a rainfall *pH* of 5.0 using Murujuga rock samples. This is in broad agreement with MRAMP thermodynamic calculations and would be equally likely under basic/alkaline conditions which appear to be as likely or more likely at Murujuga under the current environmental conditions. Whilst wet/dry deposition *pH* is more challenging as an EQC parameter as it is less closely linked to a specific emission, it is nevertheless an important environmental parameter.

A weatherability index (WI) model is under development that will permit multiple pollutant species to be combined in a singular parameter, which can be related to deposition *pH* (see Section 5). This WI is proposed to be trialled in the 2026/27 reporting period and adopted as a future EQC parameter once refined.

2.2 Chamber studies (accelerated weathering)

The MRAMP *Monitoring Studies Data Collection and Analysis Plan* (MSDCA Plan) (Curtin University, 2022) includes a series of laboratory based chamber exposure experiments. These experiments have been designed to promote accelerated weathering for the purposes of developing dose-response curves for pollutants and exposure scenarios relevant to the Murujuga airshed.

A detailed discussion of the chamber studies results and analyses to date is given in the Monitoring Studies Report 2025 (Curtin University, 2025); refer to Sections 4.4 and 7.1 in Curtin University (2025). Key points are summarised here.

The agents utilised for experiments leading to current Interim EQC have been doses of:

- gaseous NH_3
- gaseous NO_2
- gaseous SO_2

Bushfire smoke exposure experiments have also been conducted, however these have not yet resulted in EQC due to methodological issues discussed below.

In initial experiments, the combined response to each dose was defined as a combined measure of detectable elemental leaching of specified chemical elements from any of the rock samples of the five lithologies being studied (basalt, dolerite, gabbro, granite, granophyre). These response agents were measured experimentally from pre- and post- exposure samples by the ChemCentre at the highest resolution (lowest detection limit) possible for the technique applied.

The design of these experiments was informed by observations of spatial gradients in porosity, which are presented in extensive detail in the Monitoring Studies Report 2024 (Curtin University, 2024b) and Monitoring Studies Report 2025 (Curtin University, 2025).

Aluminium (Al), Calcium (Ca), Iron (Fe), Potassium (K), Magnesium (Mg), Manganese (Mn), and Sodium (Na) were measured via inductively coupled plasma-atomic emission spectroscopy (**ICP-AES**), which is a relatively sensitive technique with detection limits that range from:

- 0.001 mg/L for Mn
- 0.005 mg/L for Fe and Al
- 0.1 mg/L for Ca, Na, Mg and K.

Four elements (Ca, Na, Mg, and K) exhibited a clear dose-response relationship and were selected as the most appropriate analytes for the development of EQC, at this stage as a combined (peak normalised) response variable of Ca+Na+Mg+K concentration in pre- and post-experiment paired data. The concentration of Mn was either very low or below the limit of reporting (**LOR**) for rocks without patina, and the concentration of Fe was consistently below LOR in all samples. The concentration of Al showed variability that may be attributable to contamination by Al-bearing components in the experimental apparatus, so this element is not discussed further here. Blanks consisting of 25 mm quartz-fibre filters were utilised in the chamber and did not return detectable Al, however this element did not present a consistent trend so was omitted. This decision may be revisited in future.

Elements released into solution during the experiments were initially bound within or adsorbed externally by minerals in the rock samples prior to the experiments. The experiments used cubes of fresher rock (i.e. samples without a surface patina), so the minerals within the fresher rock are the likely sources of the elements measured by ICP-AES. The five different lithologies contain different minerals in different proportions, but Ca is likely to be released from clinopyroxene and plagioclase in the mafic (silica-poor) lithologies (basalt, gabbro, dolerite), and from plagioclase in the felsic (silica-rich) lithologies (granite, granophyre). The main Na-bearing mineral and likely

source of most of the Na for all lithologies is albite, which is an Na-rich feldspar, or plagioclase, which is an Na- and Ca-bearing feldspar, although minor Na may be released from amphiboles in the mafic lithologies. The most likely source of Mg is chlorite in all lithologies, and orthopyroxene, clinopyroxene, and amphiboles in the mafic lithologies. One of the polymorphs of alkali feldspar is the most likely source of K, although K may be held within the rock as part of clay minerals, such as illite, that form by alteration of alkali feldspar. Some proportion of all elements that are released by breakdown of the minerals present in the fresher rock at the start of the experiment may transfer to secondary clay minerals that form as part of the mineral breakdown, and this process reduces the amount of the element that is released and measured in the experimental solutions.

The LOEC was determined as the exposed dose which produced a measurable response in 30-50% of rock samples. Conversely, 50-70% of samples (rock type groups or individual sample rocks) were below LOR. While experiments in the Monitoring Studies Report 2024 (Curtin University, 2024b) indicated that reuse of rock cubes and ordering of exposures were not critical parameters in the experimental design, the Monitoring Studies Report 2025 (Curtin University, 2025) experiments with a weaker effect from the single gas exposures found these two effects appeared to be confounding. As such, experiments were redesigned to utilise ten new/fresh granophyre samples only in each test. This has permitted a dose-response relationship to be established for SO_2 and confirmation of no effect from NO_2 until what appears to be the onset of an effect at the highest achievable dose.

The LOEC from experiments was converted to a 24 hr average Standard dose, via the expression:

$$\text{Interim EQC} = \overline{\text{LOEC}_x} . \frac{t_c}{t_a} \tag{1}$$

where

$\overline{\text{LOEC}_x}$ is the mean pollutant dose concentration C_x for the experiment with the lowest observed effect concentration (LOEC),

t_c is the total duration of the (accelerated) chamber studies test, and

t_a the recalculation to a realistic field interval (one year in this case).

This conversion inherently incorporates a factor of $\sim$61 reduction (60.875 for a year length of 365.25 days) as it averages a six day dose over 12 months.

The above value is then divided by a factor of 10 to obtain an annual average guideline value. This factor is a common toxicology approach to account for synergistic effects of multiple pollutant species and other unknowns (e.g., Chapman et al., 1998).

To date, these relationships have been determined for granophyre rock samples without patina only. Future exposures will be undertaken to confirm the relationship is true for patinated rocks and basalt samples (the most reactive rock type based on calculations).

The annual average guideline Interim EQC for NH_3 is kept unchanged since the previous report (Curtin University, 2024a) as experiments using the revised methodology have not been completed at the time of writing. Likewise a 24 hr standard has not yet been developed for NH_3.

2.3 Field studies

The first Interim EQC report (Curtin University, 2024a) presented a guideline and standard for NO_2, based on a lower and upper estimate of historic NO_2 emissions and exposure. Given the lack of response to NO_2 in subsequent chamber studies, this relationship has been determined to be correlation but not causation. As shown by Henry's Law (Hites and Raff, 2012) and discussed in the Monitoring Studies Report 2025 (Curtin University, 2025), SO_2 is much more diffusive than NO_2. Therefore it is highly unlikely that the guideline represented by a green/teal line in the previous interim EQC report (Curtin University, 2024a) was causative of any impact and as such, has been removed.

Estimates of historic emissions have been amended to include an iron pellet plant which operated at Parker Point in Dampier from 1966 to 1980. This plant contributed minimal NO_2 emissions but significant SO_2 emissions (to the extent that news articles at the time documented that scrubbers for SO_2 were installed to protect workers). However, the spatial distribution patterns and levels of atmospheric SO_2 have changed significantly over time, and gas concentrations appear to have reduced faster than predicted by models (Ramboll Australia, 2020). As such, determination of cumulative historic estimates of SO_2 is a complex problem that would require extensive modelling. Historic, cumulative or peak emission of gas species (specifically, but not limited to, SO_2, from multiple sources, but likely combined with microbiome interactions) are most probably responsible for the increased porosity. However, estimation of historic SO_2 levels would be a very detailed exercise and would require information on shipping traffic and actual vs legislated fuel SO_2 data which may no longer be available. Chamber studies data and the weatherability index model are therefore the preferred approach.

2.4 Henry's Law

The Monitoring Studies Report 2025 (Curtin University, 2025) presents a discussion on Henry's Law for solubility of weak concentrations of gases in liquids. As a prelude to the weatherability index model discussion in Section 5, it is noted that the Interim EQC relationships developed to date and shown in Table 1 appear to approximately correlate with the relationships presented by Henry's Law.

2.5 Wet and dry deposition *pH*

Previous rainfall estimates were amended to include CSIRO 2006 measurements, along with data from Bednarik (2007) and MRAMP (Figure 2). These provide conclusive evidence of acidic rainfall in 2005. The bulk of these 2005 rainfall measurements fall into a range found by Neumann (2025) to cause accelerated weathering. This is in agreement with weathering calculations (see Section 5) and would equally occur at high *pH* values. As such, EQC for wet (rainfall) and dry deposition *pH* have been established, both as standards and guidelines. Appendix A-1 shows these EQC superimposed on MRAMP measurements to-date, applied to

a) rainfall samples

b) AS3580.10 total flasks

c) Wet and dry buckets from the MRAMP novel three-bucket samplers.

pH measurements from the three-bucket samplers were found to be more likely impacted by natural contamination (e.g. guano) or from rust blown in from the cage mesh of a small number of air quality monitors (**AQMs**). As such, an exceedance would be determined if two consecutive months of sampler values from one site are within either the low *pH* or high *pH* region, provided there is no evidence of sample contamination from the sources mentioned above. High *pH* values at islands such as Collier Rocks (AQ18) may be impacted by dust from carbonate bearing strata on surrounding islands (see Section 3.2).

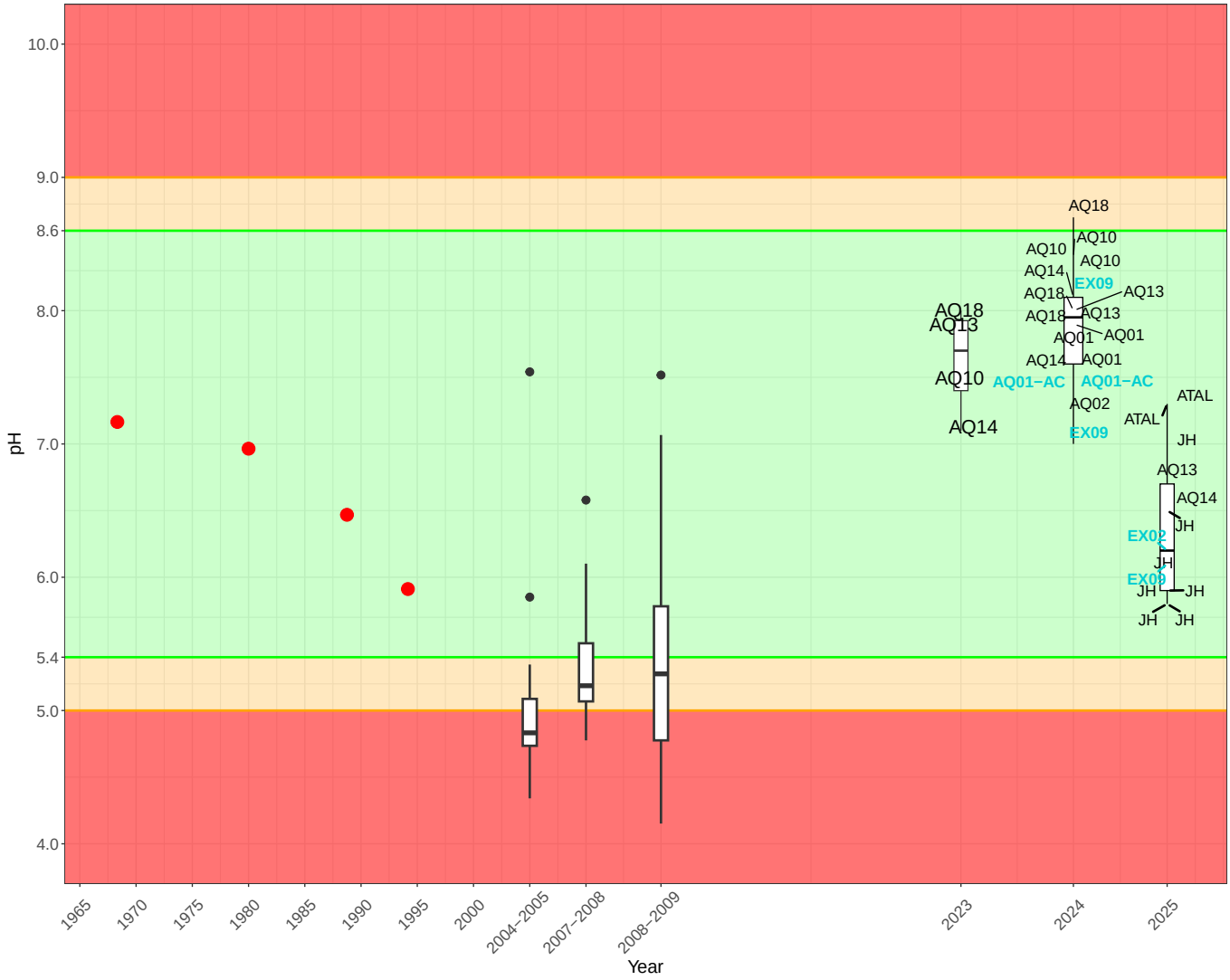

Figure 2: Application of pH EQC to historic and recent rainfall measurements. The guideline range is shown in orange and the standard in red. The red dots are digitised from Bednarik (2007). The rest of the data are presented as boxplots. 2004-2005, 2007-2008, and 2008-2009 data are from CSIRO monitoring studies report 2010. 2023 onwards are samples collected by MRAMP and analysed by Greg Skrypek, UWA. EX09, EX02, and AQ01-AC (in aqua colour) are measurements from air conditioner condensate drain samples from the powered AQMs during dry conditions. JH denotes samples collected by Professor Jo McDonald in Dampier during Tropical Cyclone Sean in January 2025.

3 Updated interim EQC

3.1 Pollutant gas species

Revised Interim EQC for gas exposures based on chamber experiments are shown in Table 1.

Table 1: Interim EQC for gas species.

Air pollutant	**Interim standard EQC**[1] **(MRAMP 24 hr avg)**		**WHO guideline**[1,2] **(24 hr avg)**		**Interim guideline EQC**[3] **(MRAMP annual avg)**		**WHO guideline**[2,3] **(annual avg)**	
	ppb	$\mu g/m^3$	**ppb**	$\mu g/m^3$	**ppb**	$\mu g/m^3$	**ppb**	$\mu g/m^3$
NO_2	219	419	13	25	22	42	5	10
SO_2	47	125	15	40	5	13	NA	NA
NH_3	-	-	NA	NA	7.4	5.2	NA	NA

Note: All values at standard temperature and pressure (STP). (1) 24 hour averages calculated from the four powered sites (AQ01, EX02, EX07 and EX09) as per the protocol for ambient air quality monitoring, see WHO or National Environment Protection Measure (**NEPM**) methods.
(2) WHO human health guideline levels are shown here for comparison purposes only.
(3) Annual averages are to be calculated monthly, based on a 12 month rolling average of IVL data for all sites. Any average that exceeds the guideline would be classified as an exceedence.

The Interim EQC in Table 1 have been developed from chamber studies that demonstrated clear dose-response relationships and calculations, literature and experimental research on weathering geochemistry.

LOECs have been determined from experiments, based on the transition to the no-effect range. These values have been utilised to develop revised Interim EQC for Murujuga, based on extrapolations established in the previous report (Curtin University, 2024a), combined with approaches to develop standard (short term peak) and long term average guideline values.

Chamber studies completed for the Monitoring Studies Report 2025 (Curtin University, 2024b) have enabled guidelines and standards to be developed for individual gas species and not combined species (NO_2 and SO_2) as per the previous iteration (Curtin University, 2024a).

The updated Interim EQC values, combined with approaches to develop short-term peak standard values and long-term average guideline values, are compared to World Health Organisation (WHO) guidelines for human health for context.

As the current Interim EQC for NO_2 and SO_2 are higher than WHO guidelines for human health, it may be preferable for the regulatory authorities to apply the WHO levels where as the study region is adjacent to the town of Dampier, which has a significant residential population. This decision is however beyond the scope of MRAMP.

It is important to emphasise the reason for the gas species EQC revision compared to the previous report (Curtin University, 2024a), particularly for NO_2.

3.2 Deposition *pH*

Separate interim EQC have been developed for wet and dry deposition *pH* based on literature studies (e.g. Neumann (2025)) and thermodynamic calculations for the Murujuga rocks presented in Section 5. These values establish guideline and standard levels for both high and low *pH* values with respect to neutral (7.0) *pH*. The high *pH* guidelines/standards are equidistant to neutral compared to the low values, supported by the weathering chemistry calculations.

Table 2 shows the proposed deposition *pH* EQC values.

Table 2: Interim EQC for deposition pH.

Parameter	Limit	EQC type	Application
Wet and / or dry deposition *pH*	<5.0 and / or >9.0	Interim Standard	All wet / dry / rainfall deposition data
Wet and / or dry deposition *pH*	5.4-5.0 and / or 8.6-9.0	Interim Guideline	All wet / dry / rainfall deposition data

An exceedance of the standard will be denoted as two consecutive months of either acidic or alkaline samples at the same site which cannot be attributed to natural causes.

Three-bucket deposition sampler exceedances should also agree with total flask deposition values for the three-bucket sampler measurement to be considered an exceedance.

Figure 2 shows the application of the *pH* EQC in Table 2 to current MRAMP rainfall *pH* data and historic data collected by others.

4 Monitoring against the Interim EQC

The monitoring program embedded in the MRAS EQMF model (Figure 1) requires each of the pollutants or environment quality indicators of concern to be measured in the field in such a way that an exceedance of an EQC Guideline or Standard level can be identified, and measures taken to manage the risk of accelerated weathering of the rock surface and damage to the rock art. Monitoring and reporting procedures are specified in detail in the *Interim Monitoring Program Design Report* (Curtin University, 2025), however the key principles are summarised here.

Prior monitoring templates will be expanded to include 24hr average data, pH and weathering index (for information only at this stage).

4.1 Monitoring locations

Figure 3 shows a map of the MRAMP air quality monitoring sites.

The MRAMP Air quality monitor / air quality monitoring (**AQM**) network includes 18 passive/solar stations (identified as AQ02 to AQ18 and AQA1), and three mains powered AQMs with real time gas analysers (AQ01 located east of Karratha, EX02 on the Dampier foreshore, and EX09 at Mt Wongama). In addition, EX07 is an existing Woodside monitoring station operated by ACOEM/Ecotech, with MRAMP owned powered instruments installed at this site.

Two temporary (limited) monitoring sites (TM01 and TM02) have been added to fill perceived “gaps” in the network and in the data interpolation/interpretation. However it is not intended for these to be used for EQC purposes at this stage as it is planned they will be decommissioned after 12-18 months of operation.

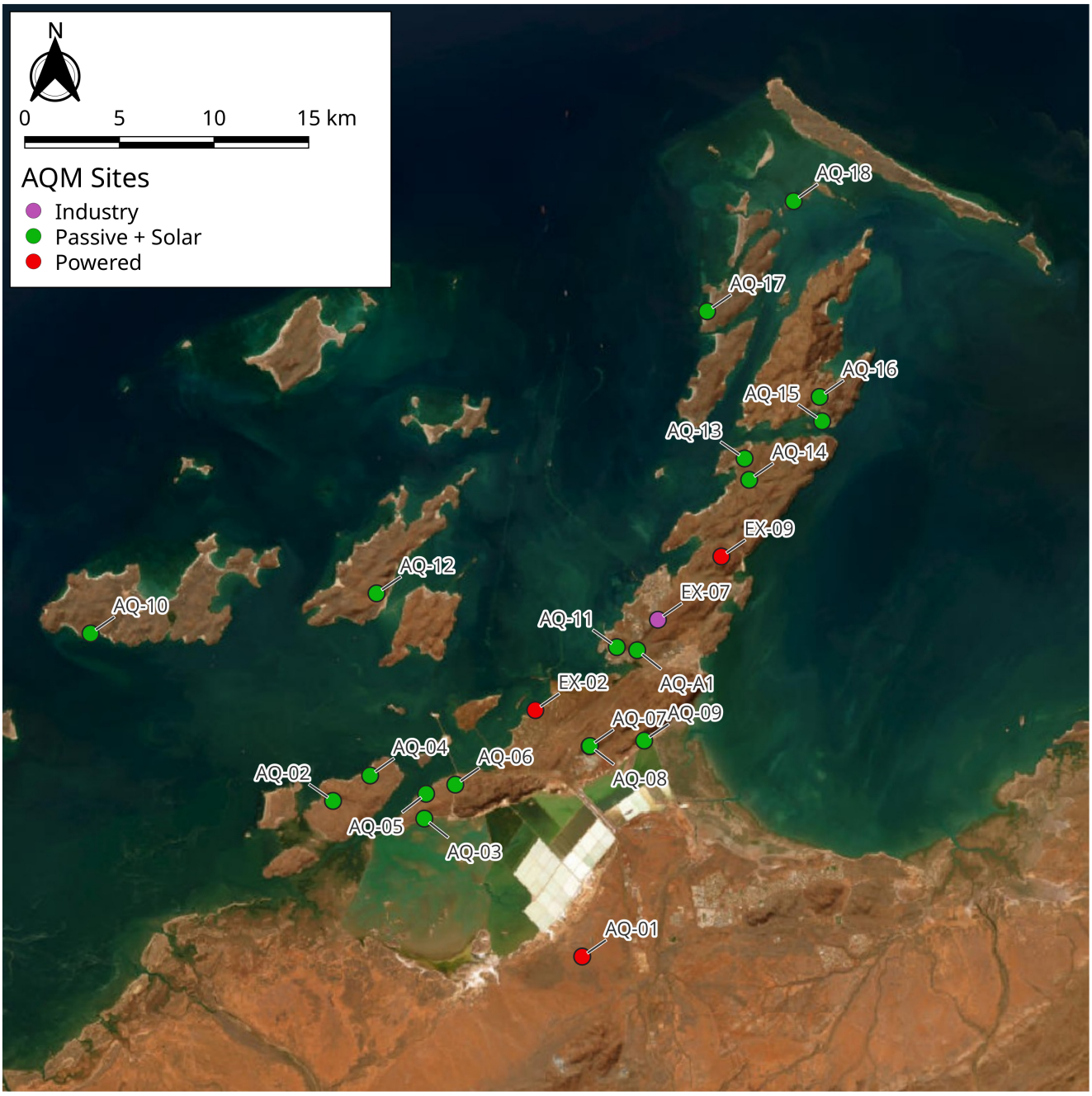

Figure 3: MRAMP Air quality monitoring sites. EX07 is a joint MRAMP/Industry site and only contains powered instruments, with no passive or deposition monitoring. The other three powered stations include passive samplers.

4.2 Annual average (passive sampler) EQC air pollutant monitoring

Continuation of the method proposed in the Interim EQC Report (Curtin University, 2024a) is recommended for monitoring and comparison with the annual average EQC parameters for each of the three pollutant gas species in Table 1, with the exception that all EQC are individual and not linked.

Monitoring will employ data collected from the passive gas samplers installed across the MRAMP air quality monitoring network. The 4-weekly average passive sampler data for each of the pollutant species will be compared against the Interim guideline EQC values defined in Table 1.

As samplers are deployed for 4-week periods and assay data are only received periodically from the (**IVL**) analytical laboratory, exceedances would be assessed and reported quarterly based on a rolling 12-month average.

4.3 24hr average (reference monitor) EQC air pollutant monitoring

A similar approach (quarterly formal reporting) will be undertaken for the 24 hr average Interim EQC values for the same three pollutant gas species in Table 1. At present, these will utilise only the high resolution powered instruments at AQ01, EX02, EX07 and EX09. These will be calculated for all 24 hr periods and reported quarterly at this stage. However, real time alerts will be implemented for early warning and corrective action if necessary.

4.4 Deposition *pH* monitoring

Monitoring against the Deposition *pH* EQC in Table 2 will be undertaken on a quarterly basis using samples collected every 4 weeks. Typical laboratory analysis time is 2 weeks, giving an 8-week lag for each monitoring cycle, allowing for report preparation. The primary measure will be the Australian Standard (AS3580.10) total flask, also termed a Dust Deposition Gauge (**DDG**). However rainfall and bucket deposition data will also be assessed and reported on a 12 month trial basis while more cross validation data is gathered. As stated above, an exceedance of a guideline or standard EQC will be determined after two consecutive months of consistent exceedance at the same site, at either the upper or lower end of the *pH* scale, that cannot be attributed to natural phenomena at the site in question. It is planned that value in any of the samplers that is higher or lower than a respective guideline or standard will be investigated. In future the 3-bucket deposition samplers may become the primary means of assessment, as results to date appear to show the three-bucket samplers have lower secondary reactions of collected phosphates and nitrates, which may alter *pH* between collection and analysis.

4.5 Weatherability index monitoring trial

Weatherability index will be calculated and reported on quarterly on a 12 month trial basis. If adopted as the primary EQC, this will likely move to a more frequent calculation and reporting cycle.

5 Combined weatherability index

5.1 Introduction

The impacts of industry-emitted reactive gases on rocks, microbes and the rock art are a complex function of multiple factors. These factors include the concentrations of the different gases and interactions amongst them in the atmosphere, seasonal variability in temperature and rainfall, and rock characteristics, such as the mineral assemblage and the reactive surface areas of those minerals. To enable comparison amongst systems where different combinations of these factors apply, a calculated parameter, the weatherability index (**WI**), was developed. This parameter does not (yet) include bioweathering.

This approach offers the advantage that the effects of multiple causes can be integrated and considered together via a single number, and provides a robust transparent method to compare amongst localities that are subject to different combinations of the influencing parameters.

The overarching criteria for the *WI* as an EQMF is that it is suitable for use with an EQMF framework. That is, the *WI* must be clear, readily measurable, and auditable, and it must be possible to devise standardised approaches for measuring and comparing the *WI* against the criteria. Rock weathering is complex and many aspects are poorly understood or only semi-quantified, so it is inevitable that simplifications must be made to satisfy the criteria around practicality and transparency for EQMF components. To be clear, these simplifications are made when information required to test and refine a more complex model does not exist. However, there is a risk that such simplifications may render the integrated formula too imprecise or insensitive to be useful, or even incorrect and misleading.

This risk must be considered in the context of the benefits of an integrated formula, which is that a semi-quantitative estimate of rock weatherability can be compared across Murujuga for any set of air quality, temperature and geological input parameters. The effects of future changes in response to, for example, improved pollution reduction technology, can also be considered. These benefits are not available if only single parameters are considered (e.g., the concentration of a single gas species), and indeed, any model linking air quality to rock weathering encounters limitations around poorly constrained rates and processes. Thus, while the limitations of the *WI* approach are acknowledged, and the specific uncertainties are discussed in detail below, the value of such an approach is considered sufficient to justify its consideration.

The interim EQC described here is a starting point that will be improved as the data sets grow, if the *WI* model is implemented. For example, the *WI* model will be tested and refined:

1. When interim EQC are converted to EQC after submission of the Y4 report. At this point the microbiome and patinated chamber studies will be complete and this information can be integrated into the model;
2. On review of the EQC after two or three years. At this point in-situ monitoring of rock art panel *pH* and patinated rock located within the AQMs will have completed two or three cycles (Curtin University, 2025), and will provide a more quantitative picture of real-time rock weathering that can be used to test, and then calibrate, the *WI* model;

3. In response to ongoing monitoring results including photogrammetry, which records flaking and other changes in rock surface condition.

5.2 Background

Rock weathering refers to changes in rocks on the Earth's surface induced by exposure to water, gases, plants, animals, free-living and symbiotic microorganisms, cycling temperature and humidity, and chemical compounds such as salts. Eventually, these processes lead to physical or chemical breakdown of the rocks to form soils, or transport of rock components from the weathering site as particulate or dissolved matter.

Weathering of rocks at Murujuga is integral to creation of the rock art. The contrast between the dark rock surface, or patina, and the paler weathered rind that underlies the patina, is only possible because of weathering that formed the patina and the weathered rind. Various engraving techniques have been used at Murujuga, however all will penetrate the patina layer and some may reach the fresh(er) rock underneath. However, weathering after rock art engraving may have a negative impact on rock art. Changes in colour may change the contrast of the art, and destabilisation of the patina, flaking of the weathered rind, or a range of other physical changes, could lead to loss of the petroglyph. Conversely, regrowth of the patina layer in the engraved area (as has occurred on what are believed to be the older petroglyphs) may obscure shallower engravings.

There are five main rock types at Murujuga: granopyhre, gabbro, dolerite, basalt, and granite (Figure 4). These are variably altered igneous rocks, mostly formed during the Archean, more than 2.6 billion years ago (Donaldson, 2011). The main rock types at Murujuga are exceptionally resistant to weathering (Pillans and Fifield, 2013), and baseline weathering at Murujuga is unusually slow, as evidenced by the preservation of rock art, up to 50,000 years old, on rock surfaces. Any acceleration of weathering rates is a concern for preservation of the rock art but such changes are challenging to recognise. It is difficult to distinguish between the integrated effects of tens to hundreds of thousands of years of non-anthropogenic weathering and those of a few decades of industrial emissions.

Fortunately, modern laboratory techniques permit micrometre- to nanometre-scale imaging of rock surfaces and sub-surfaces (Curtin University, 2024b), and these approaches have revealed spatial gradients in porosity (Curtin University, 2024b). Porosity manifests as voids below the surface of the rocks, and records dissolution of specific minerals. Mineral dissolution to form porosity is attributed to chronic exposure to emissions, most likely historic and during times of elevated emissions (Curtin University, 2024b).

Formation of porosity shows that some of the minerals that constitute the rocks at Murujuga are sensitive indicators of environmental conditions and that mineral dissolution may be a useful component of the EQMF. Further, mineral dissolution, while complex, is sufficiently well understood that process-based models can be developed to link air quality parameters to weathering rates in a quantitative way. A model of this type has been developed and described here.

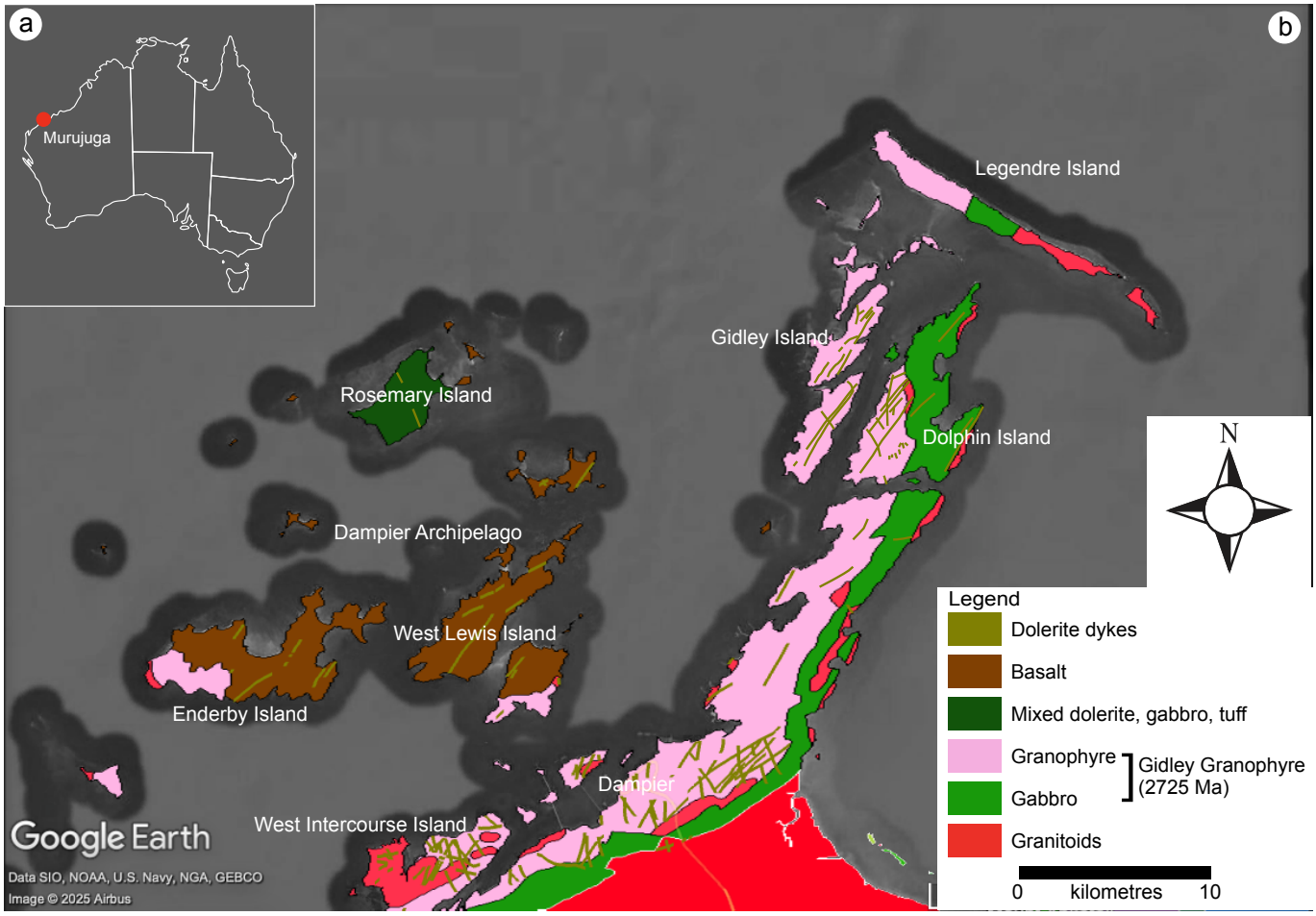

Figure 4: Simplified geological map showing solid geology. Distribution of rock types taken from the 1:250 000 interpreted bedrock geology (Hickman and Strong, 2001) and the 1:50000 Urban Geology Nickol Sheet (Australia, 1979). Map Datum:GDA2020.

5.3 Conceptual model

Mineral dissolution is a form of chemical rock weathering. The mechanisms of chemical rock weathering are complex and include surface- and transport-controlled kinetic components as well as equilibrium-controlled processes (White and Brantley, 1995). In addition, microbial bioweathering processes may enhance geochemical weathering rates (Barker et al., 1997; Wild et al., 2022). Chemical rock weathering generally requires liquid or gaseous water, and the rates and extent of mineral dissolution depends on intensive variables such as the *pH* and Eh of the coexisting aqueous phase (Blum and Stillings, 1995). These intensive variables, in turn, are defined by the concentrations of atmospheric gases, such as CO_2, and anthropogenically-produced reactive gases such as Oxides of nitrogen (NO + NO2, **NOx**) and Oxides of sulfur (SO2 + SO3, **SOx**). These reactive gases can react with water in the atmosphere or within rocks to form acids that enhance chemical weathering (Graedel and McGill, 1986). Air quality is globally heterogeneous and temporally variable, with diverse sources of emissions that have evolved with changing patterns of energy generation and improvements in air quality management (Henneman et al., 2017). Rates of rock weathering are also sensitive to rock characteristics such as grain size and mineralogy,

and climate variables such as temperature and precipitation patterns (Drever and Clow, 1995).

The first-order processes that control rock weathering are relatively well understood (e.g., White and Brantley, 1995). However, in detail, numerous interdependent processes involving multiple parameters, some of which are poorly quantified, link the composition of the atmosphere to the hydrochemistry of precipitation and the process of rock weathering (e.g., White, 1995). A complete quantitative description of these processes can be attempted if a locality is sufficiently well-characterised and monitored (e.g., Liljestrand and Morgan, 1981), but such descriptions are difficult to extrapolate because key processes show non-linear functional relationships, and require detailed site characterisation. A lack of data limits comparisons amongst localities, assessment of remote localities, and rapid assessment of the potential for changes in chemical rock weathering rates in response to changes in atmospheric chemistry. In recognition of this difficulty, previous researchers have parameterised selected components of the atmosphere–precipitation–chemical rock weathering cycle (e.g., Broomandi et al., 2022; Singh et al., 2016). While these approaches yield valuable information, the use of pre-determined constants for rock weathering rates precludes consideration of influential rock characteristics such as grain size and mineralogy, limiting their utility.

By incorporating process-based expressions for rock weathering, it is possible to devise a semi-quantitative description of weathering rates for different rock types that includes the impacts of first-order geological and atmospheric controls on chemical weathering. The output of this method is a single parameter, referred to here as the “weatherability” index (*WI*), which can be used to compare the weatherability of any rock–atmosphere system using readily available input data. This approach, subject to the limitations discussed above in Section 5.1, and below in Section 5.6.1, could be used at Murujuga as a foundation for the EQMF.

5.4 Methods

5.4.1 Weatherability index model overview and guiding principles

The model involves two steps:

- First, conversion of atmospheric gas concentrations to a proxy for rainfall *pH*.
- Second, calculation of rock weathering rates as a function of rainfall *pH*.

After these calculations, the sensitivity of any given rock to any particular suite of atmospheric conditions can be ranked according to a weatherability index (Figure 5). The term ‘system’ is used to refer to a particular rock, plus the set of atmospheric conditions (gas concentrations, precipitation rates) that coexist with the rock.

Because the model is, by necessity, simplified, it is most useful to provide a comparison amongst systems rather than to derive physically meaningful and absolute values for any given system. For example, a weatherability index of 4 may not have an instantly translatable physical meaning. However, if it increases or decreases then changes in weatherability can be used as a basis for management decisions. This consideration is fundamental to development of both steps of the model. In the conversion of atmospheric gas concentrations to rainfall *pH*, application of the model requires that the necessary data are available for every system of interest. For robust comparison, it is preferable that the data are provided by a single source, to avoid issues with

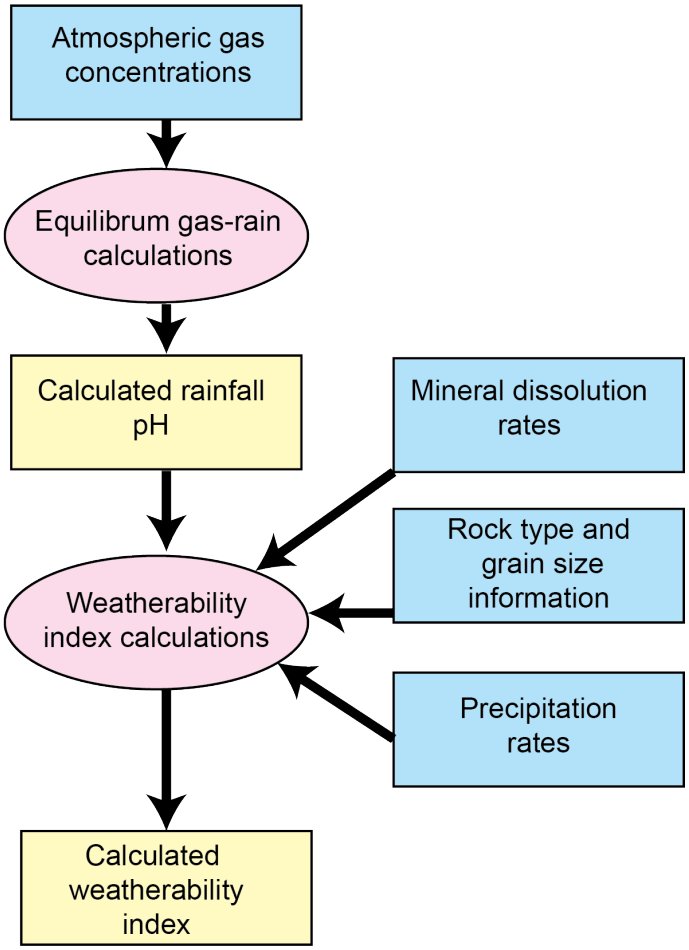

Figure 5: Conceptual model for weatherability index calculations.

different measurement techniques, different analytical accuracy and precision, and differences in the types of random and systematic errors. Similarly, it is preferable that estimates of rock weathering rates use a data set that is developed to be as close to internally consistent as possible to enable comparison for different minerals. The limitations associated with these simplifying assumptions are described below.

5.4.2 Air quality to rainfall *pH*

Atmospheric gases are described as reactive if they participate readily in chemical reactions. For example, oxides of sulfur and nitrogen (SO_x and NO_x) form sulfuric and nitric acids respectively by reaction with other atmospheric components, such as water and ozone. This process forms acid rain. Many minerals weather more quickly under acidic conditions (Palandri and Kharaka, 2004), so high concentrations of reactive gases in the atmosphere facilitate rock weathering. In addition to the acid-forming gases, reactive gases such as ammonia (NH_3), particulate silicate material (PM), and seasalt aerosols may react in the atmosphere to reduce the acidity of rainwater, mitigating the effects of acid rain.

The chemistry of the atmosphere is complex, dynamic, and dependent on a wide range of factors

(e.g., Watanabe et al., 2006). While the concentrations of some gases, such as SO_2 and NO_2, can be extracted from global monitoring databases, the data required to produce a detailed quantitative description of atmosphere chemistry for most locations are unavailable. However, following existing approaches, it is possible to calculate an estimate of rainfall *pH*, where $pH = -\log_{10}[H^+]$, from a relatively small number of reactions that involve equilibrium between atmospheric gases and water (e.g., Hites and Raff, 2012). While this *pH* is unlikely to be the actual *pH* of rainfall at the site in question because of the simplified approach, it provides a way to compare amongst systems in a robust way using readily available data.

Passive gas samplers at Murujuga measure SO_2, NO_2, NH_3, and HNO_3. These gases, along with the *pH* modification by particulate matter are considered in this simplified model, which follows Broomandi et al. (2022); Hites and Raff (2012) and Liljestrand and Morgan (1981). The equilibria considered and their equilibrium constants (K) are summarised below.

$$\begin{aligned}
\mathrm{CO_2(g)} &= \mathrm{CO_2(aq)} & KC1 &= 10^{-1.47} \\
\mathrm{CO_2(aq) + H_2O} &= \mathrm{HCO_3^-(aq) + H^+(aq)} & KC2 &= 10^{-6.35} \\
\mathrm{SO_2(g)} &= \mathrm{SO_2(aq)} & KS1 &= 100.096 \\
\mathrm{SO_2(aq) + H_2O} &= \mathrm{HSO_3^-(aq) + H^+(aq)} & KS2 &= 10^{-1.77} \\
\mathrm{NH_3(g)} &= \mathrm{NH_3(aq)} & KN1 &= 10^{1.76} \\
\mathrm{NH_3(aq) + H_2O} &= \mathrm{NH_4^+(aq) + OH^-(aq)} & KN2 &= 10^{-4.74} \\
\mathrm{2NO_2(g) + H_2O} &= \mathrm{HNO_2(aq) + HNO_3(g)} & KN3 &= 10^{-0.88} \\
\mathrm{HNO_2(aq)} &= \mathrm{H^+(aq) + NO_2^-(aq)} & KN4 &= 10^{-3.29} \\
\mathrm{H_2O} &= \mathrm{H^+(aq) + H^+(aq)} & KW &= 10^{-14}
\end{aligned}$$

5.4.2.1 *pH* calculation

The equilibrium constants for the air quality to rainfall reactions can be combined with the expression for charge balance, neglecting the concentrations of ions considered to be present in very small quantities (e.g., CO_3^{2-}).

$$(\mathrm{H^+(aq)}) + (\mathrm{NH_4^+(aq)}) = (\mathrm{HCO_3^-(aq)}) + (\mathrm{HSO_3^-(aq)}) + (\mathrm{NO_2^-(aq)}) \tag{2}$$

where round brackets indicate molar concentrations. The concentrations of each of the terms in Equation 2 can be written in terms of the equilibrium constants of the relevant reactions and the measured activities of the relevant gases, assuming ideal mixing, such that activities (square brackets) are equal to concentrations. Activities are used in Equations 3 to 6 and subsequently. The standard state for gases is the pure phase at one atmosphere, and the standard state for aqueous solutes is the hypothetical one molar solution with the properties of an infinitely dilute solution.

$$[\mathrm{HCO_3^-(aq)}] = \frac{KC1KC2[\mathrm{CO_2(g)}]}{[\mathrm{H^+(aq)}]} = \frac{K_C}{[\mathrm{H^+(aq)}]} \tag{3}$$

$$[\mathrm{HSO_3^-(aq)}] = \frac{KS1\ KS2[\mathrm{SO_2(g)}]}{[\mathrm{H^+(aq)}]} = \frac{K_S}{[\mathrm{H^+(aq)}]} \tag{4}$$

$$[\mathrm{NH_4^+(aq)}] = \frac{KN1KN2[\mathrm{NH_3(g)}][\mathrm{H^+(aq)}]}{KW} = K_{NH}[\mathrm{H^+(aq)}] \tag{5}$$

$$[\mathrm{NO_2^-(aq)}] = \frac{KN3.KN4.[\mathrm{NO_2(g)}]^2}{[\mathrm{H^+(aq)}][\mathrm{HNO_3(g)}]} = \frac{K_{NO}}{[\mathrm{H^+(aq)}]} \tag{6}$$

Rearranging Equations 2 to 6, yields

$$[\mathrm{H^+(aq)}] = \sqrt{\frac{K_C + K_S + K_{NO}}{1 + K_{NH}}}. \tag{7}$$

Adding the particulate matter term from Broomandi et al. (2022) yields

$$[\mathrm{H^+(aq)}] = \sqrt{\frac{K_C + K_S + K_{NO}}{26.12 + K_{NH}}}. \tag{8}$$

The particulate matter term has the advantage that it replicates, to some extent, increases in *pH* related to interactions between water and dust within the atmosphere. However, it is a relatively crude term that isn't sensitive to the concentration of particulate matter, so the subsequent discussion compares results with and without the particulate matter term, where relevant.

Finally, *pH* is calculated.

$$pH = -\log_{10}[\mathrm{H^+}] \tag{9}$$

As stated above, these are only a subset of the reactions that link SO_x, NO_x, and other atmospheric species to the chemistry of rainfall. In addition, the extent to which these reactions reach equilibrium depends on factors that include water droplet shape, volume, and speed of descent (e.g., Durham et al., 1981), so the use of equilibrium thermodynamic expressions, as done above, cannot replicate speciation within the system of interest. Nevertheless, this simplified set of calculations provides a way to relate atmospheric chemistry to the *pH* of rainfall, and while the absolute values calculated must be considered semi-quantitative, this approach has been shown to result in a reasonable replication of observed rainfall values (Broomandi et al., 2022; Liljestrand and Morgan, 1981; Singh et al., 2016).

It is possible to use measured dry deposition values of *pH* instead of calculated values. If the calculated and measured values are close then the choice would make little difference to the results. If the results are not close, then the measured values would normally be preferred if the measured and theoretical values are equivalent. However, dry deposition and calculated *pH* measurements are not equivalent in this case because the dry deposition measurements add a fixed amount of water to a month's accumulation of dust but without equivalent cumulative NOx and SOx exposure. The calculated *pH* simulates instantaneous equilibration of rain with atmospheric gases in their

measured concentrations. For this reason, if the measured and calculated *pH* are different then use of the lower of the values ensures that weatherability is not underestimated. Substantive differences in measured and calculated *pH* can be used to better understand this complex natural system, and as a basis for model refinement.

5.4.3 From *pH* to weatherability

Rocks are made of minerals. For example, a sandstone, which is a sedimentary rock formed on Earth's surface from particles transported by wind or water, comprises grains of minerals, (most commonly quartz), with feldspars, minor amounts of other minerals and a cement that holds the grains together. A granite is an igneous rock, formed from a magma within Earth's crust, and consists of the same minerals, but with larger grain sizes (up to several centimetres), and without cement. Other igneous rocks, such as basalt, consist of different minerals to granite. For example, basalt, gabbro, and dolerite typically include ortho- and clinopyroxenes, plus plagioclase feldspar, with or without olivine. Of these three rock types, which are referred to as mafic, basalts have the smallest grain size (typically a few tens to hundreds of micrometres), dolerites have intermediate grain sizes of a few millimetres, and the crystal grains that form gabbros range up to several centimetres in size. Metamorphic rocks, such as quartzite or soapstone, are highly variable and consist of a wide range of minerals with a wide range of grainsizes.

Any given rock typically contains more than one mineral. But, in most cases, dissolution of one of these minerals will control the degradation of a rock. For example, in an igneous rock that lacks cement, it is likely to be one of the most abundant minerals. In a sedimentary rock, which is held together by cement, it is likely to be the cementing mineral. Once the cementing mineral has dissolved, the constituent grains of the sedimentary rock no longer adhere to each other and the rock disintegrates. For this reason, one mineral for each rock type at Murujuga is selected, and that mineral is considered to control the rate of rock degradation. While K-feldspar is typically more common than the plagioclase feldspars in unaltered granite and granophyre, the extensive hydrothermal alteration has converted much of the K-feldspar to albite. In addition, the plagioclase feldspars dissolve more quickly than K-feldspar. Rate-controlling primary minerals are summarised in Table 3.

Table 3: Summary of minerals considered to control the rate of rock weathering in the five rock art hosting rock types at Murujuga.

Rock type	Minerals
Granite	Plagioclase
Granophyre	Albite
Gabbro/Dolerite/Basalt ($pH < 6$)[1]	Clinopyroxene
Gabbro/Dolerite/Basalt ($pH > 6$)[1]	Plagioclase (labradorite)

[1] The rate-controlling mineral for the mafic rocks (gabbro/dolerite/basalt) is different at *pH* values higher and lower than six.

The calculations presented here describe dissolution of the substrate for the engraved rock art. In many cases, rock art visibility is provided or enhanced by the contrast between a dark layer of patina, also referred to as rock varnish, and paler underlying rock (Dorn, 2020). Dissolution

or rapid regrowth of the patina would have negative impacts for rock art preservation, but is not considered here for two main reasons:

- First, current concerns around the preservation of rock art at Murujuga are based on reports that found elevated porosity, attributed to mineral dissolution, within the uppermost millimetres of the rock substrate to the rock art, focusing investigation on this layer (Curtin University, 2024b, 2025).
- Second, patina is mineralogically and compositionally complex, with strong variability on the micrometre-scale. Patina systems are dynamic on timescales that are not yet well understood, and host a diverse but poorly understood microbiome. Recent advances in patina understanding are helpful (Curtin University, 2024b; Neumann et al., 2022; Neumann, 2025), but are not yet sufficient for quantitative descriptions of patina formation and destruction.

For these reasons, it is difficult to predict the impacts of atmospheric gases on patina in a quantitative way using existing information. However, observations of the patinated rock billets, which will be mounted in the AQMs (Curtin University, 2025), will provide detailed annual observations of the well-characterised patina, reducing uncertainties related to inter-sample variation. It is possible that this information can be integrated into the *WI* model, enabling consideration of this critical component of the rock surface.

A further complexity is that mineral dissolution can be congruent or incongruent. If mineral dissolution is congruent then every element within the mineral forms an aqueous species on dissolution, so the mineral dissolves entirely. If mineral dissolution is incongruent then only some of the elements in the mineral form aqueous species while some of the less soluble elements (e.g., Si, Al) are retained and form a new mineral or a leached and degraded form of the original mineral. Clays are a common product of incongruent dissolution. The widespread distribution of clays within the weathered rind at Murujuga indicates that incongruent dissolution operates to some extent within the weathering rind. For this reason, it is, on first sight, appealing to include incongruent dissolution within the WI approach. However, the rates and characteristics of the processes that form and subsequently modify clays are not well known and a semi-quantitative parameterisation of those processes of the type undertaken here is difficult to test. Further, clays are rheologically weak compared to their precursor minerals, so clay formation reduces the strength of the rock such that physical weathering of a clay-rich rock is fast relative to physical weathering of a fresher rock on Murujuga. Finally, SEM-BSE images of the outer layers of many of the rocks show that the lower parts of the weathered rind are richer in clay minerals than the upper parts, where voids are more common (Curtin University, 2024b). This indicates that the clay dissolution zone, which can be visualised as a volume that separates the region where clays are dominantly weathered out of the rock from the region where clays are more common than voids, advances more quickly than the mineral dissolution zone, which separates the fresher rock from the region where most of the fresher rock minerals have been replaced by clays. This observation indicates that chemical weathering of clays is faster than chemical weathering of the precursor fresher rock minerals.

For this reason, weathering of the precursor minerals listed in Table 3 is considered to provide the dominant control on weathering leading to disintegration of the rock. While this is a simplification, it still enables a robust first-order comparison amongst systems because the same approach can be applied to each regardless of whether a detailed study of mineral dissolution at that site has already been performed.

Mineral dissolution rates depend on the mineral characteristics, temperature, pressure, and the concentration of dissolved ions within the dissolving aqueous phase. Protons (H^+) are typically considered the most influential ion for mineral dissolution rates (Palandri and Kharaka, 2004), and conveniently mineral dissolution rates derived from experiments are typically formulated as a function of *pH* (Palandri and Kharaka, 2004). If *pH* is known, then mineral dissolution rates can be calculated in units of moles per m^2 of mineral per second, providing an opportunity to link atmospheric chemistry to mineral dissolution via *pH*. Expressions of this type describe surface-controlled mineral dissolution (Berner, 1978).

Surface-controlled dissolution rates of common minerals have been investigated experimentally for a range of conditions (e.g., Bennett, 1991; Brantley and Chen, 1995; Johnson et al., 1998). The results of laboratory experiments have been parameterised for use in software packages that can simulate mineral dissolution in environmental and geological systems (e.g., Parkhurst and Appelo, 2013). Here we use the database of Palandri and Kharaka (2004). In this compilation, mineral dissolution rates are parameterised as the sum of terms for dissolution under acidic, neutral, and basic conditions, to allow for the different reaction mechanisms that dominate under different *pH* conditions. The parameterisation is described in detail in Palandri and Kharaka (2004) and summarised briefly here. Equation 10 expresses the dissolution rate as the sum of acid, neutral, and basic terms.

$$\frac{dm}{dt}_{\text{total}} = \frac{dm}{dt}_{\text{acid}} + \frac{dm}{dt}_{\text{neutral}} + \frac{dm}{dt}_{\text{basic}} \tag{10}$$

where $\frac{dm}{dt}$ is the change is the number of moles of a mineral with respect to time for unit surface area, with units of moles m^{-2} s^{-1}. Each of these terms is formulated as an Arrhenius equation, such that, for example,

$$\log \frac{dm}{dt}_{\text{acid}} = \log A_{\text{acid}} - \frac{E_{\text{acid}}}{2.3025 \text{R} T} - n_{\text{H}^+,\text{acid}}\, pH, \tag{11}$$

where:

- A is the Arrhenius pre-exponential factor (mol m^{-2} s^{-1});
- E is the activation energy in kJ mol^{-1};
- T is the temperature in Kelvin;
- $n_{\text{H}^+,\text{acid}}$ is the reaction order with respect to protons for the acid term (e.g., Oelkers and Schott, 1995); and
- R is the gas constant (0.008314 kJ mol^{-1}).

Palandri and Kharaka (2004) present values for A, E, and $n_{\text{H}^+,\text{acid}}$ for a range of common minerals, based on a comprehensive compilation of experimental mineral dissolution rates. Some of the tabulated values are presented as $\log k_{298.15,0}$ and E, where the $\log k_{298.15,0}$ value is the dissolution rate at *pH* equal to 0 and 298.15 K. The value of A can be calculated from $\log k_{298.15,0}$ and E via

$$\log A = \log k_{298.15,0} + \frac{E}{2.3025 \times 298.15 \times R}, \tag{12}$$

based on Equations 5 to 7 of Palandri and Kharaka (2004), noting an error in their Equations 6 and 7.

Experimental dissolution rates are up to several orders of magnitude faster than mineral dissolution rates in natural environments (e.g. Drever and Clow, 1995). Discrepancies have been attributed to hydrological, temperature, *pH*, and particle size factors (e.g., Drever and Clow, 1995; Malmstrom et al., 2000). These factors are accounted for to some extent here, via the grain size and precipitation factors, which are described below. These adjustments are not considered quantitative but do permit robust comparison amongst the sites considered.

5.4.3.1 Grain size factor

The surface area of a mineral exposed to a dissolving solution is one of the most important mineral characteristics that affects dissolution rates (e.g., Brantley and Chen, 1995). For example, a rock made of 1 mm diameter grains of a given mineral dissolves more quickly than a rock made of 1 cm diameter grains of the same mineral because the total mineral surface area of the finer-grained material is greater. If the relative surface area and duration of mineral dissolution can be parameterised then the weatherability can be calculated.

Here, we assume that the rock is made of spherical grains of radius r. The volume of a grain is 4/3 πr^3, and the surface area is $4\pi r^2$. If grains are close packed, then 0.7408 of a volume is occupied by grains (Wu et al., 2003), and the number of grains in a unit volume is $\frac{0.7408}{4/3\pi r^3}$, with a total surface area of 2.2224/r. Thus, the surface area factor (SAF) is defined as

$$SAF = \frac{2.2224}{r} \tag{13}$$

This approach is a simplification. Features such as cleavage, non-spherical grain shapes, variably developed porosity, and fractures mean that the effective surface area is different to the calculated surface areas by an amount that is unknown. Further, the reactive surface area of minerals depends on the mineral itself. For example, the reactive surface area of a clay mineral is vastly greater than that of a pyroxene of equivalent grain size. However, uncertainties introduced by these complexities are considered unlikely to be greater than the orders of magnitude differences in surface area that relate to grain size–volume relationships. However, it is possible to perform effective surface area measurements on the Murujuga rocks to reduce this source of uncertainty. This work will be recommended if the interim EQCs are retained in a form similar to that proposed here.

5.4.3.2 Precipitation factor

Generally, water is necessary for minerals to dissolve. Water can be present as grain boundary films formed by condensation or fog, or as precipitation, and dry deposition contributes to rock degradation (Graedel and McGill, 1986). A comprehensive quantification of these complexities is not possible without detailed meteorological records for each site, which are not available, so weathering is proportional to a precipitation factor (PCP) which is defined by

$$PCP = \frac{\text{yearly precipitation at site } (\text{mm year}^{-1})}{\text{reference yearly precipitation } (\text{mm year}^{-1})} \tag{14}$$

The absolute value of the reference yearly precipitation doesn't affect the relative values of weatherability because the factor is logged to obtain the weatherability index. This means that the reference value is a constant that is subtracted from the other parts of the calculation and affects every site equally, but it is required to render PCP dimensionless.

5.4.3.3 Normalisation to one oxide

Different minerals have different formula, such that, for example, one mole of quartz (SiO_2) has a different amount of material to one mole of K-feldspar ($KAlSi_3O_8$), which means that dissolution of one mole of quartz would release only one mole of Si, whereas dissolution of one mole of K-feldspar would release three moles of Si, as well as one mole of each of K and Al. To account for this difference, the dissolution rate of each mineral in moles m^{-2} s^{-1} ($\frac{dm}{dt}_{\text{total}}$ from Equation 10) is divided by the number of oxides in the mineral formula, so

$$\frac{dm}{dt}_{\text{one oxide}} = \frac{1}{n_{\text{ox}}} \frac{dm}{dt}_{\text{total}} \tag{15}$$

where n_{ox} is the number of oxygen equivalents in a mineral formula.

5.4.3.4 Weatherability index

Combining Equations 10 to 15, the weatherability index, *WI*, is defined as

$$WI = 10 + \log \frac{dm}{dt}_{\text{one oxide}} + \log SAF + \log PCP. \tag{16}$$

High values indicate high weatherability and vice versa. The weatherability index forms a log scale, so an increase in the weatherability of one unit indicates increased dissolution rates by a factor of 10, and vice versa.

5.5 Application of the weatherability index

The weatherability index was applied to the different rock types of Murujuga under conditions recorded at selected MRAMP AQMs. Reactive gas concentration inputs were taken from the IVL passive sampler data for each AQM. Average monthly precipitation and temperatures were taken from the Bureau of Meteorology records for Karratha Aero station (004083). If this methodology is retained then future applications of this technique will be able to use temperature and precipitation records from the individual AQMs, which better reflect the variability of weather conditions across Murujuga.

5.5.1 Predicted *pH*

Rainfall *pH* was calculated using Equations 2 to 9 for three selected AQMs (AQ01, AQA1, AQ17) using the IVL passive sampler data (Figure 6a). Calculated *pH* values were less than the measured values, indicating that the calculation provides a conservative lower estimate of rainfall *pH*, and confirming that this technique can be used for comparison but not to predict absolute values to be used for comparison with the proposed EQC *pH* values. One possible reason for the discrepancy is that rainwater may have interacted with clay particles within the atmosphere, increasing *pH* (e.g., Broomandi et al., 2022). The effect of particulate matter on rainfall *pH* was investigated by Broomandi et al. (2022) for UNESCO world cultural heritage sites in Eastern Asia. Rainfall *pH* values calculated with and without the particulate matter term derived by Broomandi et al. (2022) were compared (Figure 6b). Inclusion of the PM term increases calculated *pH* values by up to 0.1 unit, but not to values as high as those observed. Further work is necessary to establish whether a different PM term is more appropriate for Murujuga, and to assess the impacts of other possible contributors to the difference between observed and calculated *pH* values.

5.5.2 Comparison of rock types

The weatherability index was calculated for AQM site AQ01 using IVL passive sampler data, Equations 2 to 16, and average monthly precipitation and temperature values from the Bureau of Meteorology for the Karratha Aero station (004083) (Figure 7). This site is not associated with rock art but was selected because it does not record the higher NO_2 values measured proximal to industry on Murujuga, or the elevated SO_2 values recorded proximal to shipping sources of SO_2 emissions.

Values range from slightly negative values for gabbro, the slowest weathering lithology, during the dryest and coldest times of year, to values of around three for basalt during the wettest and warmest times of year. This difference implies that weathering rates vary by a factor of 1000. The order of weatherability is generally consistent with observations of patina thickness. For example, gabbro generally shows the thickest patina while patina on basalt is typically thin or absent. This finding confirms the importance of the weathered rind for rock art conservation and longevity.

It is also interesting to compare the relative weatherability with the abundance of rock art on each rock type. The distribution of rock art today reflects a combination of the rates of rock art production and loss. Multiple factors contribute to whether a particular rock surface of a particular rock type was selected as the site for rock art production. For example, large relatively flat surfaces, which are most commonly provided by granophyre, may have been attractive for rock art. In addition, the orientation of surfaces, degree of surface colouration, presence/absence of patina, position within the landscape, and proximity to resources such as water are likely to have been influential.

Indeed, granophyre, which is the most abundant rock type, hosts the highest number of rock art sites (Donaldson, 2011). Gabbro is the second most abundant rock type, and host the second-highest numbers of rock art sites. Typically, gabbro is rougher than granophyre, making rock art production more difficult. However, gabbro also tends to have a thicker patina than granophyre, so that rock art could be inscribed deeply. In contrast, basalt has a smooth surface, but rock art on basalt is sufficiently rare that is difficult to find.

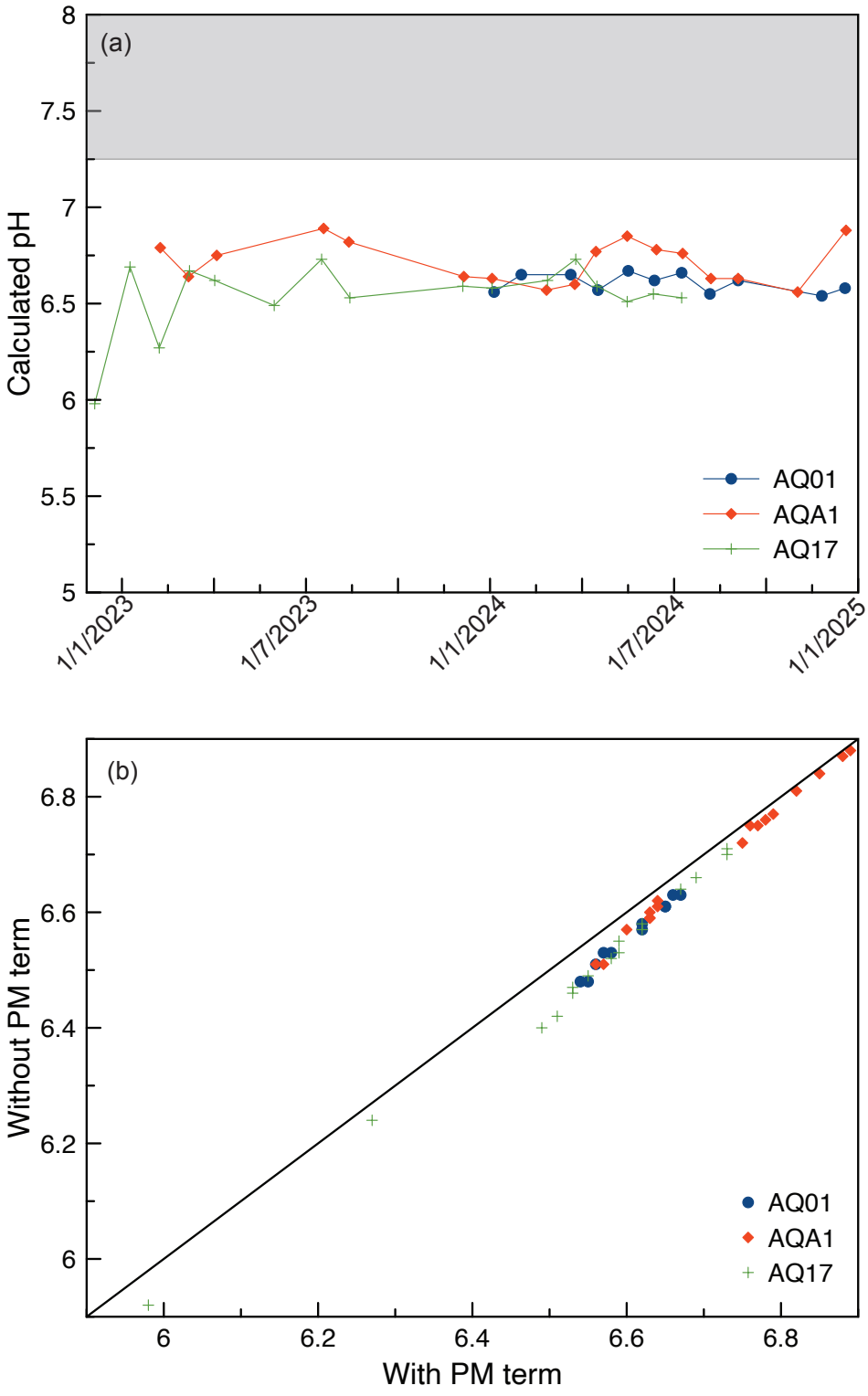

Figure 6: Rainfall pH values calculated using MRAMP passive air quality sampler data and the weatherability index model. Panel (a) shows a comparison of calculated rainfall pH for sites AQ01, AQA1, and AQ17 as a function of time. The grey box indicates measured pH values. Panel (b) shows a comparison of calculated pH values for sites AQ01, AQA1, and AQ17 with and without the particulate matter term.

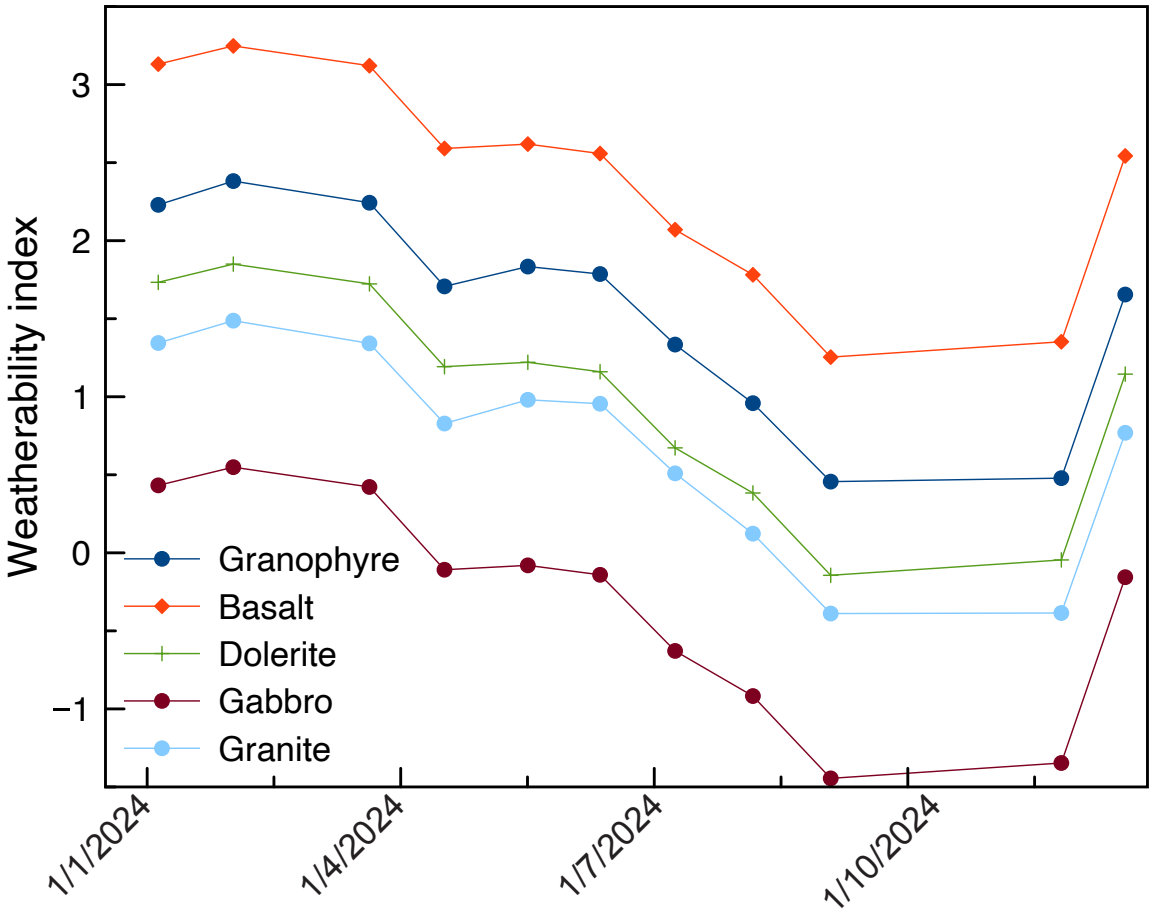

Figure 7: Calculated weatherability as a function of rock type for site AQ01 as a function of time.

The *WI* is directly related to the rate of rock art loss. Therefore, it is possible to speculate that the high proportion of rock art on granophyre, and the low proportion on basalt reflects, to a greater or lesser extent, the low *WI* of granophyre and the high *WI* of basalt, as well as other factors discussed above.

5.5.3 Comparison of weatherability index amongst global World Heritage sites with petroglyphs

The weatherability index was calculated for 29 sites that are World Heritage-listed for petroglyphs (Figure 8). Input air quality data for these sites were obtained from the Copernicus Atmosphere Monitoring Service (**CAMS**) and rock type information was obtained from the UNESCO World Heritage listing descriptions, supported by geological maps. The CAMS data do not provide NH_3 so that term was omitted, but do provide NO, so the expression was slightly different to that shown above, but the comparison amongst sites is considered valid.

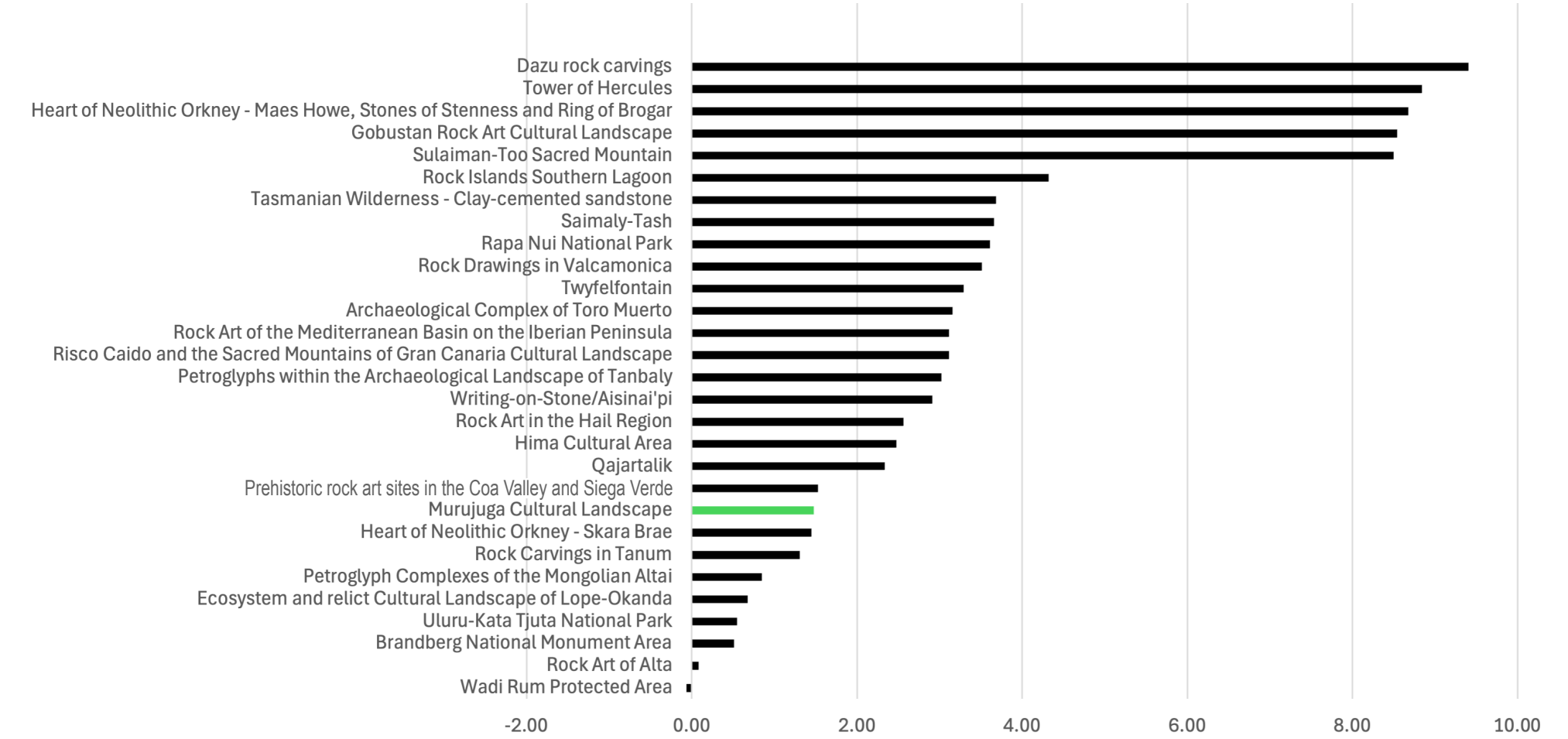

Figure 8: Calculated weatherability index for 29 World Heritage sites where the Outstanding Universal Value could be impacted by surface weathering. The value for Murujuga is for granophyre and is shown in green. The term for NH_3 was omitted from the calculations because the CAMS measurements don't provide NH_3.

5.5.4 Comparison of weatherability index amongst MRAMP AQMs

The weatherability index was calculated and compared for granophyre and basalt at AQM sites AQ01 (average SO_2 = 0.24 μg m^{-3}), AQA1 (average SO_2 = 0.33 μg m^{-3}), and AQ17 (average SO_2 = 1.38 μg m^{-3}) using the monthly IVL passive sampler data (Figure 9). Rainfall and temperature data were taken from the Bureau of Meteorology data for Karratha Aero (004083). The weatherability index can be calculated for any lithology at any site, regardless of whether that lithology exists at that site, using the average grain-size and mineralogical information for that lithology derived from previous work (Curtin University, 2023, 2024b).

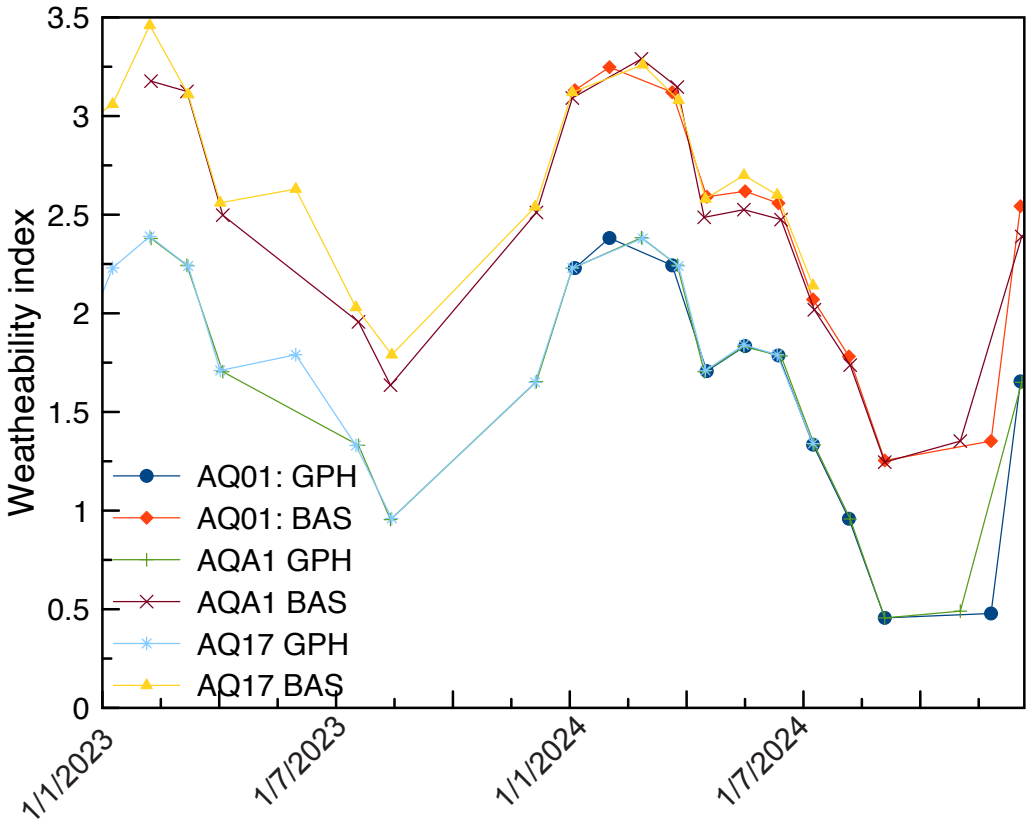

Figure 9: Calculated weatherability index for AQM sites AQ01, AQA1, and AQ17 using IVL passive sampler data.

Site AQA1 was selected because it yields some of the highest concentrations of reactive gases other than SO_2. Site AQ17 was selected because it yields some of the highest measured SO_2 concentrations. Site AQ01 was selected because it does not record the higher NO_2 values measured proximal to industry on Murujuga, or the elevated SO_2 values recorded proximal to shipping sources of SO_2 emissions. There are no rocks or rock art at site AQ01 and the rock characteristics used in the model (grain size, mineralogy) were taken from those for the specified rock types elsewhere on Murujuga.

Calculated weatherability indices range from 0.5 to 3.5, a variation of three orders of magnitude. The lowest values were calculated for granophyre at times of low rainfall and temperature, highlighting the sensitivity of the systems to climate parameters. The highest values were calculated for basalt at site AQ17, at the time of highest recorded SO_2, confirming that the model is sensitive to the

concentrations of reactive atmospheric gases. Most of the variability relates to rock type and precipitation; the consistent difference of around 0.75 units between granophyre and basalt is explained by differences in rate-controlling mineral and grain size. The difference of around two units between January 2024 and September 2024 relates mostly to changes in precipitation rate, with temperature playing a smaller role. Changes in gas concentrations are relatively small, so they do not induce large changes in *WI*.

It is interesting to compare variations of this magnitude to the variation amongst World Heritage sites (Figure 8). *WI* values of around 0.5, similar to those calculated from granophyre at the driest times of year, are calculated for the Brandberg National Monument Area in the arid Namib Desert, which is ranked second lowest of the thirty sites considered. A *WI* value of around 3, similar to those calculated for basalt at the wettest times of year, are calculated for petroglyphs within the archaeological landscape of Tanbaly, Kazakhstan, where petroglyphs were created on clay-cemented sandstone, which weathers slightly slower than basalt but the rainfall, SO_2, and NO_2 concentrations are higher than those at Murujuga.

Notwithstanding this sensitivity, calculated weatherability indices for all three sites are similar for any given rock type. This result indicates that rock type, temperature, and precipitation are first order controls on calculated weatherability under current conditions. Of these factors, precipitation and rock type provide stronger effects than temperature (not shown). The effect of changes in the concentrations of atmospheric gases is second order. It is difficult to see how these second order changes could account for the increased porosity observed proximal to industry on Murujuga (Curtin University, 2024b, 2025), based on present-day emissions.

5.5.5 Historic weatherability index estimates at Murujuga

Relationships amongst the concentrations of SO_2, NH_3, HNO_3, and NO_2 on calculated *pH* and *WI* were investigated (Figures 10 and 11). The intention of this investigation was to assess the effects of historical and future changes in emissions on calculated *pH* and *WI*. To investigate the effects of the gases individually, all gas concentrations except the gas of interest were set to the average concentration measured by the IVL passive samplers for monitoring station AQ01 during 2024. The concentration of the gas of interest was varied from 10% of its current value to 1,500 $\times$ the current value in ten steps. The *pH* and *WI* were calculated for each step using Equation 7.

None of the simulations produced *pH* values as low as those reported by the CSIRO 2006. At this time, NH_3 emissions were lower than those today because the fertiliser plants were not operating. To investigate these conditions, NH_3 concentrations were set to 0.001 $\mu g/m^3$, and SO_2 was varied from 10% of its current value to 1500 $\times$ the current value in ten steps (0.024 to 3.6 $\mu g/m^3$) (Figures 10a and 11a).

Calculated *pH* decreases from 6.62 to 6.22 with increasing SO_2 values at current NH_3 concentrations, and from 5.62 to 5.26 under low NH_3 concentrations (Figure 10a). This difference highlights the complexity and contrasting impacts of different atmospheric gases. Basalt is much more sensitive to changes in calculated *pH* than granophyre. At current levels of NH_3, increasing SO_2 induces an increase in *WI* of basalt from 2.6 to 2.81, implying an increase in weathering rate of 58% (Figure 11a). At low NH_3 levels, the *WI* of basalt increases from 3.2 to 3.45 with increasing SO_2 concentrations. While the change in weathering rate induced by changing SO_2 is significant, the absolute change related to changes in NH_3 is greater by almost a factor of five.

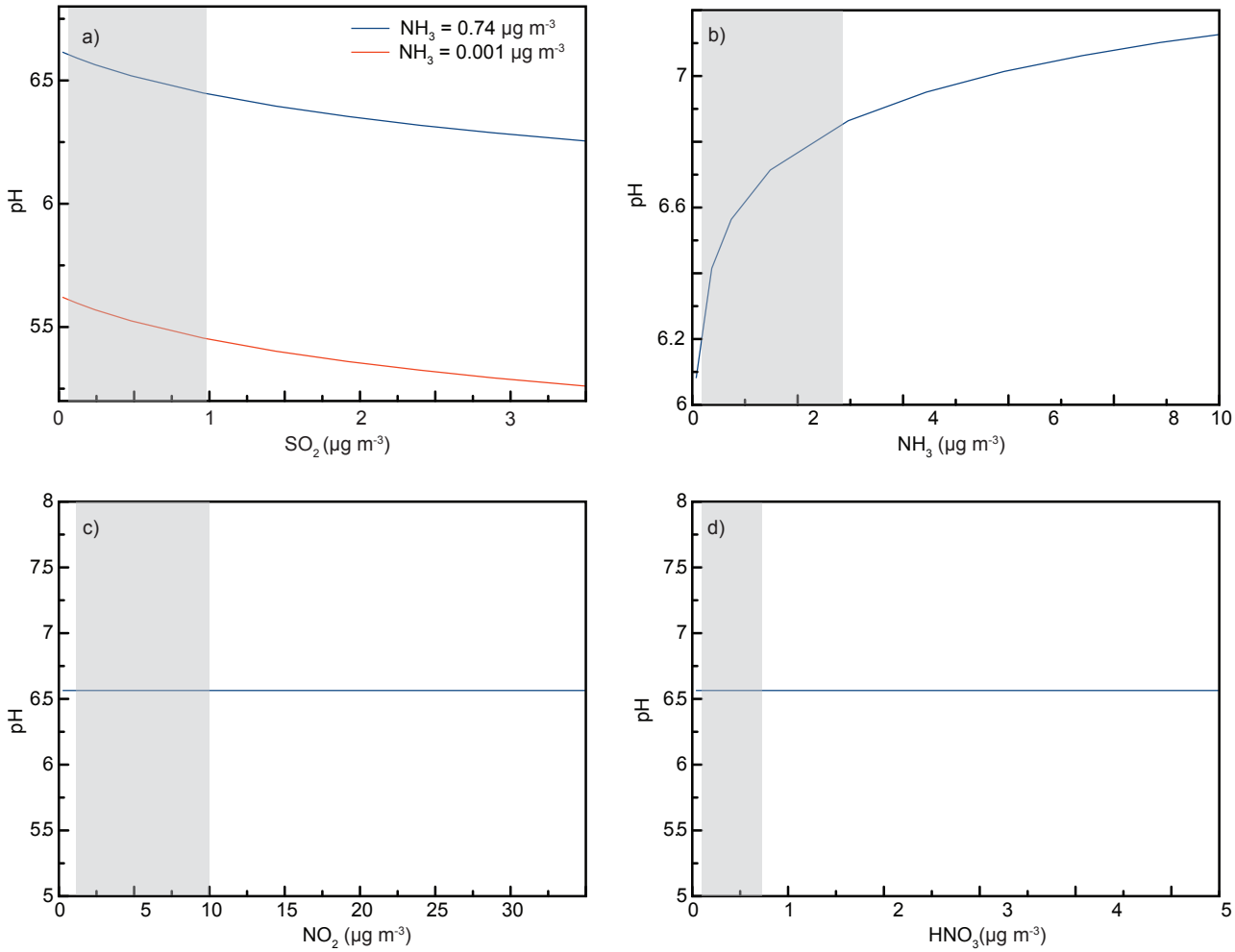

Figure 10: Calculated pH for elevated values of reactive gases. Unless otherwise stated, gas concentrations other than that shown on the x axis have been set to the average levels measured by the IVL passive gas samplers at AQ01 during 2024. Grey boxes approximate the range of current measurements by passive gas samplers across all AQMs, omitting rare high SO_2 measurements at AQ17. Panel (a) shows the effect of increasing SO_2 with and without current NH_3 levels. Panel (b) shows the effect of increasing NH_3. Panel (c) shows the effect of increasing NO_2. (d) Panel (d) shows the effect of increasingHNO_3.

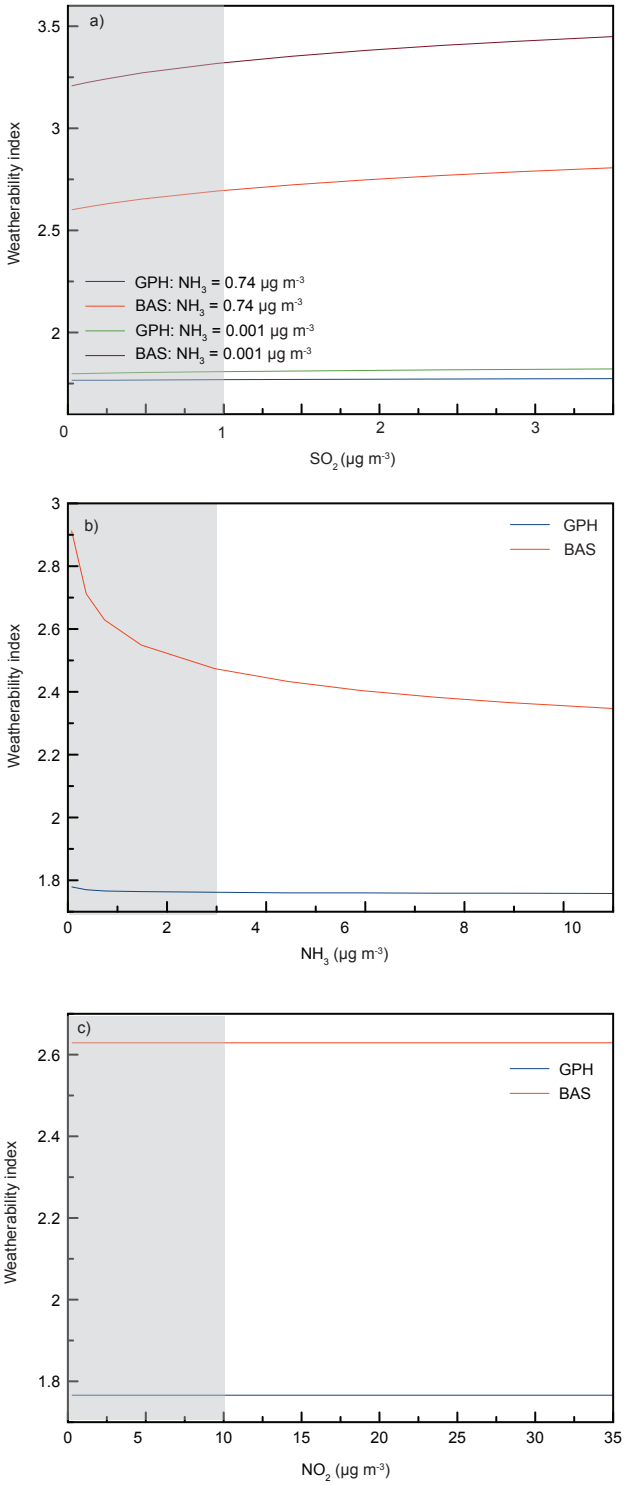

Figure 11: Calculated WI for elevated values of reactive gases. Notes: (1) Unless otherwise stated, gas concentrations other than that shown on the x axis have been set to the average levels measured by the IVL passive gas samplers at AQ01 during 2024. (2) Grey boxes approximate the range of current measurements by passive gas samplers across all AQMs, omitting rare high SO_2 measurements at AQ17. (3) Panel (a) shows the effect of increasing SO_2 with and without current NH_3 levels. Panel (b) shows the effect of increasing NH_3. Panel (c) shows the effect of increasing NO_2.

With increasing NH_3, calculated *pH* increases from 6.08 to 7.15 (Figure 10b), and the *WI* decreases from 1.78 to 1.76 for granophyre, and from 2.91 to 2.35 for basalt (Figure 11b). At first sight, this result indicates that NH_3 slows rock weathering. However, mineral dissolution rates increase with increasing *pH* once conditions become alkaline, and NH_3 may also have effects on rock weathering that are linked to its effects on the microbiome. These effects are under investigation.

Neither *pH* nor *WI* are sensitive to NO_2 or HNO_3 (Figure 10c,d and Figure 11c). This may reflect an oversimplified approach to these atmospheric species, or it may reflect that rainfall *pH* is much less sensitive to these species than to SO_2 and NH_3, as stated by Singh et al. (2016) and Broomandi et al. (2022).

5.5.6 Effect of maxima and minima in reactive gas concentrations

The calculations above are based on data from the IVL passive samplers, which provide concentrations averaged over a month of data collection. The powered AQM sites provide continuous monitoring of gas concentrations, and maxima and minima in these data were used to provide instantaneous maxima and minima in calculated rainfall *pH* and *WI*. Gas concentrations other than the concentration of interest were set to the average levels measured by the IVL passive gas samplers at AQ01 during 2024. Precipitation and temperature were set to the average yearly values for Karratha Aero (004083), taken from the Bureau of Meteorology. Rainfall *pH* and *WI* were calculated for granophyre (GPH) and basalt (BAS) (Table 4). Rainfall *pH* values were calculated without and with the particulate matter term (Equations 7 and 8, respectively).

The calculated values of rainfall *pH* range from 5.54 (minimum NH_3, no particulate matter) to 7.62 (maximum NH_3, with and without particulate matter) (Table 4). Changes in SO_2 from current averages to maximum decreased *pH* by about half a unit. A decrease in SO_2 to minimum values increased *pH* by 0.06 of a unit. These changes are independent of whether the particulate matter term is included. The calculated values of rainfall *pH* are essentially independent of variation in atmospheric NO_2 concentrations.

Calculated values of *WI*, using calculated *pH* values without the particulate matter term, range from 1.75 to 1.80 for granophyre, and from 2.19 to 3.26 for basalt. Minimum values were calculated for maximum NH_3 concentrations and vice versa. Changes in SO_2 from current averages to maximum increased the *WI* by about 0.01 and 0.3, for granophyre and basalt, respectively. A decrease in SO_2 to minimum values decreased the *WI* by less than 0.01 and by 0.03 for granophyre and basalt respectively. The calculated values of *WI* are essentially independent of variation in atmospheric NO_2 concentrations.

5.6 Weatherability index EQC development

Results of calculated rainfall *pH* and *WI* indicate that this approach has potential as a basis for an EQC for Murujuga. Calculated values are sensitive to atmospheric gas concentrations, and the weatherability index can be calculated readily for any set of IVL data anywhere on Murujuga. Incorporation of rock characteristics, such as grainsize and mineralogical information, and other environmental parameters, such as rainfall and temperature, permits a holistic view of rock dissolution that combines the relevant observations into a conveniently calculated and easily understood monitoring parameter.

Table 4: Calculated pH and WI for maximum and minimum concentrations of SO_2, NH_3, and NO_2 measured by the continuous monitors at the powered AQM sites during 2025.

Case	**SO_2**	**NH_3**	**HNO_3**	**NO_2**	***pH* PM**	***pH* no PM**	***WI* GPH**	***WI* BAS**
Units	$\mu g/m^3$	$\mu g/m^3$	$\mu g/m^3$	$\mu g/m^3$				
Max SO_2	9.480	0.740	0.381	2.503	6.11	6.06	1.78	2.92
Max NH_3	0.240	94.860	0.381	2.503	7.62	7.62	1.75	2.19
Max NO_2	0.240	0.740	0.381	2.503	6.61	6.56	1.77	2.63
Min SO_2	0.000	0.740	0.381	28.930	6.67	6.62	1.77	2.60
Min NH_3	0.240	0.000	0.381	2.503	6.25	5.54	1.80	3.26
Min NO_2	0.240	0.740	0.381	0.019	6.61	6.56	1.77	2.63

5.6.1 Improvements to the weatherability index model

The *WI* model can be used as it is, as a semi-quantitative description of rock weatherability that can be used to assess the relative impacts of environmental factors. However, as discussed above, the model is subject to limitations on our knowledge of the rates and processes that determine rates of rock weathering. Application of a *WI* model as part of the EQMF would benefit from a number of improvements that can be undertaken if the approach is deemed useful. These include:

- Inclusion of a term to simulate weathering during times of dry deposition. One way to do this in a process-based way using well established formulations is to add a diffusion-controlled term to the surface-reaction controlled terms that are already incorporated into the model.
- Inclusion of a term to simulate the effects of atmospheric gases on microbiome-facilitated mineral dissolution. Microbial metabolism is likely to be accelerated in the presence of elevated concentrations of N and S-bearing compounds, but the form and magnitude of this effect is not well known (e.g., Uroz et al., 2009). Chamber experiments are in progress to establish the form of a microbial term and better determine the parameters that control the weathering of the rocks of Murujuga. Results of these chamber experiments and other monitoring may be used to derive the approximate form and order of magnitude of such a term. These data will be available for integration into the model for the Y4 report.
- Better formulation of the particulate matter term. The particulate matter term of Broomandi et al. (2022) is effectively a constant, so calculated *pH* values are independent of the amount of particulate matter. The comprehensive datasets collected for Murujuga provide an opportunity to derive a more complex and, consequently more precise and accurate particulate matter term.
- Better descriptions of oxidation of reactive gases in the atmosphere. The equilibrium-based description of interactions amongst atmospheric gases and water (Equations 2 to 9) does not include oxidation of SO_2 to sulfuric acid, or oxidation of NO_2 to nitric acid. The relatively good agreement amongst calculated and observed *pH* values, and systematic underestimation of *pH* by the equations indicate that the expressions used provide a conservative estimate of the formation of acid rain. However, such terms would be necessary to calculate the low *pH* values recorded by Department of Environment and Conservation, Western Australia (2006). Equilibrium expressions for HNO_3 dissolution and dissociation were tested in early versions of the *WI* model but predicted values of *pH* around 3. Such acidic rain is not recorded at

Murujuga, so the equilibrium model is considered inadequate to describe NO_2 oxidation, which is a highly dynamic and kinetically controlled processes. Subsequent iterations of the model may include such terms.

- A term to describe the effects of soot. Soot and other bushfire products have been shown to impact rock coatings (e.g., Dorn, 2020), and the *pH* of rock surfaces (Curtin University, 2024b). Soot is formed by bushfires, and, with climate change, may become more important as a driver for rock:atmosphere processes at Murujuga. Soot concentrations can be measured and their effects included.
- Incorporation of terms to describe patina dissolution and modification. The use of a *WI* model based on the substrate to the patina is somewhat justified by the qualitative field observations that patina is thin or absent on basalt, which is predicted to be the fastest dissolving lithology, and thickest on gabbro, which is predicted to be the slowest dissolving lithology (Figure 7). This observation indicates that substrate stability is a first order control on patina thickness. If patina thickness is proportional to its age, which is reasonable given that patina is largely externally derived, then substrate stability is also a first order control on rock art preservation. However, patina preservation is also critical to rock art stability, so inclusion of patina-forming minerals such as the Fe- and Mn-oxyhydroxides would be a useful addition to the *WI* model. The data required to integrate patina into the *WI* model do not yet exist but will be produced by the long term monitoring of patinated billets proposed in Curtin University (2025).
- It is possible that small local-scale variations in rock characteristics affect rates of rock weathering. Such variations include changes in rock texture, mineralogy, degree of natural weathering, and the micro-environment. These factors may contribute to the preservation potential of a petroglyph. The data required to integrate these factors into the *WI* model do not exist yet, but will be produced by the long term monitoring of patinated billets proposed in Curtin University (2025). Many years may be required for weathering to proceed sufficiently to produce significant changes so this could be a longer term objective.

5.6.2 Application of a weatherability index model

It is useful to consider how a *WI* model could be applied. The *WI* parameter is formulated on a log scale, so changes in *WI* of 0.1 imply changes in dissolution rate of around 25% relative. While this increment is small, given the very low dissolution rates at Murujuga, such a change, for fixed precipitation and temperature values, should be measurable and may be appropriate as an interim guideline value. Changes in *WI* of 0.2 imply changes in dissolution rate of around 60% relative. Such an increment may be acceptable as a monitoring criteria for Murujuga. These increments are consistent with historic changes in *WI* that have been linked to local porosity development (Curtin University, 2024b).

According to the *WI* calculations, basalt is the fastest weathering lithology at Murujuga (Figures 9 and 11). Basalt is predicted to weather rapidly because its grain size is small, maximising the surface area term, and dissolution of this lithology is controlled by the rate of dissolution of clinopyroxene at *pH* values less than 6 (Table 3). Clinopyroxene is the fastest-dissolving of the rate-controlling minerals at Murujuga. Basalt is present mostly on the outer islands, and rock art is relatively rare on basalt. The paucity of rock art on basalt may relate to the relatively fast weathering of this lithology. The sensitivity of basalt provides an opportunity to use this lithology for monitoring as proposed in Curtin University (2025).

The *WI* model has applications beyond assessment of the impacts of local industrial emissions. Factors that are affected by climate change, such as temperature and precipitation, and CO_2 concentrations, are already incorporated into the model. Climate change is expected to increase the incidence of bushfire, and the impacts of bushfire-related atmospheric species could be added, as discussed above. Some parameters are affected by local and global factors; changes in global SO_2 emissions have led to better air quality but reduced earth albedo, exacerbating the impacts of rising CO_2 on global temperatures. The sensitivity of the *WI* model to these factors provides a method that can be used to assess changes in rock weathering rates related to climate change. The *WI* model is sufficiently versatile that it can be used to assess the impacts of climate change on rock art at Murujuga and elsewhere. However, we note that there is always a balance between increasing complexity, which renders models more site specific and increased data requirements, and increasing general applicability. As presented, the *WI* model has general applicability, but future refinements, such as the integration of a term for the microbiome, may render it more precise and sensitive, but less generally applicable.

6 Summary

The updated Interim EQC established in this report (see Section 3) will continue to be reviewed and refined as research work progresses. It is anticipated that all current EQC will be revised in the future and may be combined into a single weatherability index (as described in Section 5), which will permit a larger number of agents to be considered.

The EQC values will remain as Interim EQC until the final year of MRAMP research is complete. As per the specifications in the MRAS, the Final EQC from the current research program will be subject to periodic review and revision as further monitoring data are collected over time (DWER, 2019b). These reviews are likely to be based on analyses of rock art and sample rock condition monitoring. Final EQC will encompass both guideline and standard levels as shown schematically in Figure 1 and will be applied as per the EQMF specification to ensure the environmental values of Murujuga are protected (DWER, 2019a).

It is important to note that owing to the complex nature of the rock surface weathering processes taking place at Murujuga and the prolonged timescale over which (non-anthropogenic) weathering occurs, it may not be possible to develop EQC values for all gaseous species present in the Murujuga airshed that would typically be considered criteria air pollutants (**CAP**). This is because CAP have been selected largely based on human health effects. Some of these pollutants are:

- unlikely to impact the rock/microbiome
- not present above trace levels at Murujuga, or
- naturally occurring in the rock/mineral structure (e.g. lead (Pb)).

However, the weatherability index approach (see Section 5) gives a means of combining all pollutant species known to influence *pH*.

7 Glossary and abbreviations

Table 5: Glossary.

Term	Definition
Airshed	A geographical region with a common flow of air or over which air pollutants are dispersed.
Anthropogenic	From human activity. In the context of this research anthropogenic includes human impact, including industrial, transport, tourism, site management, and all other impact that can be attributed to human activity. It can also be considered to include distal or global human activity which may impact the natural environment through changes in climate.
AQM	Air quality monitor/air quality monitoring.
AQMs	Air quality monitors.
Arrhenius relation	The Arrhenius equation describes the exponential dependence of the rate constant of a chemical reaction on the absolute temperature.
Biofilm	A biofilm growing on a surface typically comprises a syntrophic (feeding together) consortium of microbial cells that are embedded in a slimy extracellular matrix that is composed of extracellular polymeric substances (EPSs). The organisms that live close together can “communicate” with each other (share nutrients, exchange genes to make them immune to antibiotics etc.). In some cases a biofilm can comprise a single species of microbial cells, however biofilms in environmental contexts typically involve multiple microbial species.
Bioweathering	The degradation of mineral/rock surfaces through biological mechanisms. Some examples include organic/inorganic acid production, physical alterations from hyphae growing into rock surfaces and metabolic processes resulting in the release of metals from the rock, and/or formation of new minerals.
Boxplot	The middle line (inside the box) is the median (50% of the data); the lower bound of the box is the lower quartile (first 25% of the data) and upper bound of the box is the third (75% of the data) quartile; “whiskers”(values at which the horizontal lines stop) are approximately 95% confidence interval; data points greater or lesser than the termination of the whiskers are outliers.
CAMS	Copernicus Atmospheric Monitoring Service.
CAP	Criteria Air Pollutants are six common air pollutants which statutory or regulatory authorities in most regions are generally required to monitor - primarily for human health considerations. These are: ozone, particulate matter, carbon monoxide, lead, sulfur dioxide, and nitrogen dioxide.
Culturally Important Place or Site	A location that has been identified as having cultural significance to Traditional Owners and Custodians that may be due to the existence of archaeological, ethnographic, historic, natural or social values. This includes values that may or may not be tied to a specific feature or geographic point in the landscape and may include tangible or intangible features tied to specific points in the landscape or a broader area or landform unit.
DDG	Dust Deposition Gauge.

Term	Definition
Detection Limit (DL) or Limit of Detection (LOD)	Lowest quantity of a substance that can be determined directly or derived from a measurement signal.
Dispersion	The spreading out of emissions from a localised source (e.g. industry stack, wildfire) over a wide area due to the effect of wind.
DWER	Department of Water and Environmental Regulation.
Eh-pH	A parameter which indicates the stability of mineral or chemical systems based on the activity of hydrogen ions (*pH*) and electrons (*Eh*). These are often compared using an *Eh-pH* diagram (Pourbaix diagram).
EQC	Environmental Quality Criteria include both “Standard” and “Guideline” EQC (EPA, 2016; EPA, 2017). The former represent limits above which sufficient evidence exists that impacts are likely to occur (to appropriate levels of confidence), whereas the latter represents EQC which are set to level where effects could theoretically occur - so as to ensure appropriate early warning such that emissions can be reduced before Standards are reached. EQC may monitor dose (e.g. air pollutants) or response (rock/art) parameters.
EQMF	Environmental Quality Management Framework - a framework to guide the assessment and management of activities related to a particular environmental value.
Fresher rock	Rock that does not show weathering alteration.
Geochemical Biomarkers	Organic compounds produced from natural degradation of biochemicals produced by living organisms or compounds produced through biosynthesis of actively growing microbes. The structure of a biomarker can sometimes be linked to a biochemical produced by a specific organism or group of organisms, while others are more general.
Heterotrophs	Heterotrophic bacteria and fungi that derive energy from organic compounds.
ICP-AES	Inductively coupled plasma-atomic emission spectroscopy.
IVL	IVL Svenska Miljöinstitutet AB / Swedish Environmental Research Institute, also refers to passive samplers designed and analysed by IVL. Sometimes referred to as “Ferm” samplers as they were developed primarily by Dr M. Ferm
LOEC	Lowest observed effect concentration (LOEC).
LOR	Limit of reporting. The lowest concentration of a substance/chemical which can be reliably reported by a laboratory.
MAC	Murujuga Aboriginal Corporation.
Microbiome	An integrated community of micro-organisms (bacteria, archaea, microbial eukaryotes and fungi) occupying a particular habitat.
Microcolonial fungi	A specific group of Fungi that are growing in microcolonial form and typically have thick cell walls and dark pigmentation. They are highly resistant against desiccation and ultraviolet damage.
Mineral assemblages	Presence and abundance of mineral species in a given spatial region (either across the rock surface or from the rock surface to the “fresh” rock below the outer weathered rind).

Term	Definition
MRAS	Murujuga Rock Art Strategy.
Murujuga	Traditional name for Burrup Peninsula and surrounding islands of the Dampier Archipelago.
MRAMP	Murujuga Rock Art Monitoring Program - includes initial studies to inform the design of the ongoing monitoring framework, as well as the development of EQC and the EQMF. Following completion of the studies, the program will transition to ongoing monitoring.
NOEC	No observed effect concentration (NOEC).
Ongoing monitoring	The ongoing monitoring refers to the longer-term monitoring program to be jointly run by MAC and DWER once the current program of works is complete. Also referred to as “long-term monitoring”.
Organic geochemistry	The study of organic compounds in the environment, including in rocks, sediments, soils, petroleum, aquatic environments and the atmosphere. Organic geochemistry studies the origin of organic compounds, their transportation processes, and the alteration they undergo in the environment, over time scales ranging from the present day to hundreds of millions of years ago.
NH_3	Ammonia.
NO_2	Nitrogen dioxide.
NO_x	Oxides of nitrogen (NO + NO_2).
Patina	In the Murujuga context the texture and colour of the rock surface is referred to as a patina. This is a deliberately broad definition, which encompasses the full spectrum of rock surface characterisation, including rock varnish, desert varnish or biological matter. It also includes any other exposed, highly weathered rock surface and biota/biofilms/biological residue which may be present on the surface. The patina has been shown to form over a depletion zone, referred to as the crust or weathered rind. Weathered rind generally has a lighter appearance than both the patina and the underlying rock. An engraving is formed by breaking through the naturally formed patina to expose the lighter crust beneath. There may be cases where the engraving is deep enough to expose the underlying rock, which in this case may result in a darker engraved channel. There are many examples where a fully developed patina/varnish layer has regrown in engraved grooves. These examples are generally considered among the oldest petroglyphs for this reason.
Permeability	A measure of how easily a fluid (e.g. air) can move through connected pores/voids in an otherwise solid material. A material composed of closed pores (e.g. a closed cell foam) would have porosity without permeability. Rock permeability is typically measured using a permeameter, which passes a known volume of air through the sample while measuring pressure.
Petroglyph	Literally “rock mark”, the term describes any cultural marking into a rock surface. The marks can be produced by a range of techniques, including pecking, pounding, incising, scratching or abrading, or a combination of two or more techniques. Techniques such as scratching can be very shallow ($<$1 mm), while pecking can be from 1 mm to more than 100 mm deep. All petroglyphs at Murujuga are Culturally Important.

Term	Definition
Photoautotrophs	Photoautotrophs are organisms that can make their own energy using light and carbon dioxide via the process of photosynthesis. Examples are cyanobacteria and green algae, known to colonise rock surfaces. Photoautotrophs are considered primary producers since their biomass can be consumed by heterotrophs (defined above) as a source of carbon and energy.
Photolysis	The process by which molecules are broken down into smaller molecules by exposure to sunlight (typically UV radiation).
PM	Particulate matter.
p-value	A statistical measure used in evaluating the strength of evidence. First a "null hypothesis" is formulated. After data are obtained, the p-value is defined as the probability of obtaining data at least as extreme as the data that were obtained, where this probability is calculated under the assumption (for the sake of argument) that the null hypothesis is true. A small p-value is interpreted as evidence against the null hypothesis, because if the p-value is very small, then "either something very unlikely has happened, or the null hypothesis is false". In this report, following standard conventions, a p-value $<$0.04 is deemed 'statistically significant' evidence against the null hypothesis.
Porosity	The void space in an otherwise solid material. Usually represented as a ratio of void volume to total volume. Rock porosity can be measured using a range of techniques including scanning electron microscopy from thin sections and micro-Computed Tomography from larger samples.
SO_2	Sulfur dioxide.
SOx	Oxides of Sulfur (SO_2 + SO_3).
Three bucket deposition sampler	The three bucket deposition sampler is a novel sampler designed for MRAMP which splits deposition samples into dry, wet (rain) and mist/dew samples. The Australian standard method (AS3580.10) uses a single (total) deposition flask which combines all conditions into a single sample.
Weathered rind	The portion of the rock between the surface (patina) layer and the fresher inner rock. This layer is sufficiently close to the surface to have interacted with oxygen or other environmental conditions. The weathered rind is significantly thicker than the surface patina layer and has different colouration to the underlying fresher rock (core).
Weathering	In the Murujuga context the concepts of weathering are differentiated as natural weathering and accelerated/anthropogenic weathering, which may be termed "degradation" to distinguish it from natural weathering. However, these effects may be difficult to decouple. • Natural weathering: the alteration of a rock surface through natural agents such as the impacts of temperature cycles, microbial activity, and interactions with water and aerosols/gases released by the surrounding (natural) terrestrial and marine environments. Weathering may be subtractive (erosion) or additive (mineralisation or accretion). • Accelerated weathering: degradation due to anthropogenic activity over and above the rate of natural weathering.
WI	"Weatherability" index - A calculated parameter that describes the relative sensitivity of a rock unit to weathering for specified concentrations of reactive atmospheric gases.

8 References

Australia, G. S. o. W. (1979). Nickol bay - legendre urban geology map 1:50000.

Bai, Z. and Yan, Y. (2025). Dose–Response Functions for Assessing Corrosion Risks to Urban Heritage Materials from Air Pollution Under Climate Change: Insights from Europe and China. *Buildings*, 15(13):2271.

Barker, W. W., Welch, S. A., and Banfield, J. F. (1997). *Biogeochemical weathering of silicate minerals*, volume 35 of *Reviews in Mineralogy*, pages 391–428.

Bednarik, R. G. (2007). The science of Dampier rock art–Part 1. *Rock Art Research*, 24(2):209–246.

Bennett, P. C. (1991). Quartz dissolution in organic-rich aqueous systems. *Geochimica Et Cosmochimica Acta*, 55(7):1781–1797.

Berner, R. A. (1978). Rate control of mineral dissolution under earth surface conditions. *American Journal of Science*, 278(9):1235–1252.

Blum, A. E. and Stillings, L. L. (1995). *Feldspar dissolution kinetics*, volume 31 of *Reviews in Mineralogy*, pages 291–351.

Brantley, S. L. and Chen, Y. (1995). Chemical weathering rates of pyroxenes and amphiboles. *Chemical Weathering Rates of Silicate Minerals*, 31:119–172.

Broomandi, P., Jahanbakhshi, A., Fathian, A., Darynova, Z., Janatian, N., Nikfal, A., Kim, J. R., and Karaca, F. (2022). Impacts of ambient air pollution on UNESCO world cultural heritage sites in Eastern Asia: Dose-response calculations for material corrosions. *Urban Climate*, 46:101275.

Chapman, P. M., Fairbrother, A., and Brown, D. (1998). A critical evaluation of safety (uncertainty) factors for ecological risk assessment. *Environmental Toxicology and Chemistry*, 17(1):99–108.

Curtin University (2022). *Murujuga Rock Art Monitoring Program: Monitoring Studies Data Collection and Analysis Plan*. Report prepared by Curtin University for the Murujuga Aboriginal Corporation and Department of Water and Environmental Regulation, Government of Western Australia (COPP21065-PLN-G-102_0). Government of Western Australia. https://www.wa.gov.au/government/publications/murujuga-rock-art-monitoring-program-monitoring-studies-data-collection-and-analysis-plan.

Curtin University (2023). *Murujuga Rock Art Monitoring Program: Monitoring Studies Report 2023*. Report prepared by Curtin University for the Murujuga Aboriginal Corporation and Department of Water and Environmental Regulation, Government of Western Australia (COPP-21065-REP-G-101). Government of Western Australia. https://www.wa.gov.au/government/publications/murujuga-rock-art-monitoring-program-monitoring-studies-report-2023.

Curtin University (2024a). *Murujuga Rock Art Monitoring Program: Interim Environmental Quality Criteria*. Report prepared by Curtin University for the Murujuga Aboriginal Corporation and the Department of Water and Environmental Regulation, Government of Western Australia. Published in 2025.

Curtin University (2024b). *Murujuga Rock Art Monitoring Program: Monitoring Studies Report 2024*. Final Report prepared by Curtin University for the Murujuga Aboriginal Corporation and the Department of Water and Environmental Regulation (COPP21065-REP-G-105). Government of Western Australia. Published in 2025.

Curtin University (2025). *Murujuga Rock Art Monitoring Program: Monitoring Studies Report 2025*. Draft Report prepared by Curtin University for the Murujuga Aboriginal Corporation and the Department of Water (COPP21065-REP-G-109). Government of Western Australia. Revision C.

Department of Environment and Conservation, Western Australia (2006). *Burrup Peninsula Air Pollution Study: Final Report*. Report Submitted to WA DOIR Rock Art Committee.

Department of Water and Environmental Regulation (2019a). Murujuga Rock Art: Environmental Quality Management Framework. Technical report. Department of Water and Environmental Regulation, Government of Western Australia.

Department of Water and Environmental Regulation (2019b). Murujuga Rock Art Strategy: A monitoring, analysis and decision-making framework to protect Aboriginal rock art located on Murujuga (the Dampier Archipelago and Burrup Peninsula). Technical report. Department of Water and Environmental Regulation, Government of Western Australia.

Department of Water and Environmental Regulation (DWER) (2021). *Murujuga Rock Art Monitoring Program: Conceptual Model* [Fact sheet]. Government of Western Australia. https://www.wa.gov.au/government/publications/murujuga-rock-art-monitoring-conceptual-model.

Donaldson, M. (2011). Understanding the rocks: Rock art and the geology of Murujuga (Burrup 'Peninsula'). *Rock Art Research*, 28(1):1–9.

Dorn, R. I. (2020). Anthropogenic interactions with rock varnish. *Biogeochemical Cycles*, 34(3):e267–283.

Drever, J. I. and Clow, D. W. (1995). Weathering rates in catchments. *Chemical Weathering Rates of Silicate Minerals*, 31:463–483.

Durham, J. L., Overton, J. H., and Aneja, V. P. (1981). Influence of gaseous nitric-acid on sulfate production and acidity in rain. *Atmospheric Environment*, 15(6):1059–1068.

Environmental Protection Authority (2016). *Technical Guidance: Protecting the Quality of Western Australia's Marine Envrionment.* https://www.epa.wa.gov.au/sites/default/files/Policies_and_Guidance/TechnicalGuidance_ProtectingTheQualityOfWAMarineEnvironment-131216_0.pdf.

Environmental Protection Authority (2017). *Environmental quality criteria reference document for Cockburn Sound*. A supporting document to the State Environmental (Cockburn Sound) Policy 2015. https://www.epa.wa.gov.au/sites/default/files/Policies_and_Guidance/EQCRefDocforCockburnSoundFeb2017-2.pdf.

Graedel, T. E. and McGill, R. (1986). Degradation of materials in the atmosphere. *Environmental Science & Technology*, 20(11):1093–1100. doi: 10.1021/es00153a003.

Henneman, L. R. F., Liu, C., Mulholland, J. A., and Russell, A. G. (2017). Evaluating the effectiveness of air quality regulations: A review of accountability studies and frameworks. *Journal of the Air & Waste Management Association*, 67(2):144–172.

Hickman, A. and Strong, C. (2001). Dampier-barrow island, western australia sheet sf50-2, 1:250000 geological series.

Hites, R. A. and Raff, J. D. (2012). *Elements of Environmental Chemistry*. Wiley, New Jersey.

Johnson, J. W., Knauss, K. G., Glassley, W. E., DeLoach, L. D., and Tompson, A. F. B. (1998). Reactive transport modeling of plug-flow reactor experiments:: quartz and tuff dissolution at 240 degrees c. *Journal of Hydrology*, 209(1-4):81–111.

Liljestrand, H. M. and Morgan, J. J. (1981). Spatial variations of acid precipitation in southern california. *Environmental Science & Technology*, 15(3):333–338.

Malmstrom, M. E., Destouni, G., Banwart, S. A., and Stromberg, B. H. E. (2000). Resolving the scale-dependence of mineral weathering rates. *Environmental Science & Technology*, 34(7):1375–1378.

Neumann, J. T. (2025). *Experimental weathering of Aboriginal rock art from the Murujuga Peninsula, Western Australia: Do emissions from the local industry have an impact on the rock art weathering rate?* Phd thesis, University of Bonn, North Rhine-Westphalia, Germany.

Neumann, J. T., Black, J. L., Hœrlé, S., Smith, B. W., Watkins, R., Lagos, M., Ziegler, A., and Geisler, T. (2022). Artificial weathering of rock types bearing petroglyphs from Murujuga, Western Australia. *Heritage Science*, 10(1):77.

Oelkers, E. H. and Schott, J. (1995). Experimental study of anorthite dissolution and the relative mechanism of feldspar hydrolysis. *Geochimica Et Cosmochimica Acta*, 59(24):5039–5053.

Palandri, J. and Kharaka, Y. K. (2004). A compilation of rate parameters of water-mineral interaction kinetics for application to geochemical modelling. Report, U.S. Geological Survey and National Energy Technology Laboratory.

Parkhurst, D. and Appelo, C. (2013). Description of input and examples for PHREEQC version 3 – A computer program for speciation, batch-reaction, one-dimensional transport, and inverse geochemical calculations.

Pillans, B. and Fifield, L. K. (2013). Erosion rates and weathering history of rock surfaces associated with aboriginal rock art engravings (petroglyphs) on burrup peninsula, western australia, from cosmogenic nuclide measurements. *Quaternary Science Reviews*, 69:98–106.

Ramboll Australia (2020). Study of the cumulative impacts of air emissions in the Murujuga airshed. Technical report. `https://www.wa.gov.au/government/publications/study-of-the-cumulative-impacts-of-air-emissions-the-murujuga-airshed`.

Singh, S., Elumalai, S. P., and Pal, A. K. (2016). Rain estimation based on the particulate matter pollutants and wet deposition study. *Science of the Total Environment*, 563:293–301.

Uroz, S., Calvaruso, C., Turpault, M. P., and Frey-Klett, P. (2009). Mineral weathering by bacteria: ecology, actors and mechanisms. *Trends in Microbiology*, 17(8):378–387.

Visone, F., Abate, N., Sileo, M., and Masini, N. (2025). Assessing stone material recession of cultural heritage: New approach based on satellite-based rainfall data and dose-response functions—case of UNESCO Site of Matera. *Remote Sensing*, 17(8):1443.

Watanabe, K., Takebe, Y., Sode, N., Igarashi, Y., Takahashi, H., and Dokiya, Y. (2006). Fog and rain water chemistry at Mt. Fuji: A case study during the september 2002 campaign. *Atmospheric Research*, 82(3-4):652–662.

White, A. F. (1995). *Chemical weathering rates of silicate minerals in soils*, volume 31 of *Reviews in Mineralogy*.

White, A. F. and Brantley, S. L. (1995). *Chemical weathering rates of silicate minerals: An overview*, volume 31 of *Reviews in Mineralogy*, pages 1–22.

Wild, B., Gerrits, R., and Bonneville, S. (2022). The contribution of living organisms to rock weathering in the critical zone. *npj Materials Degradation*, 6:98.

Wu, Y., Fan, Z., and Lu, Y. (2003). Bulk and interior packing densities of random close packing of hard spheres. *Journal of Materials Science*, 38:2019–2025.

A Appendix

A-1 Application of the new *pH* EQC to existing MRAMP data

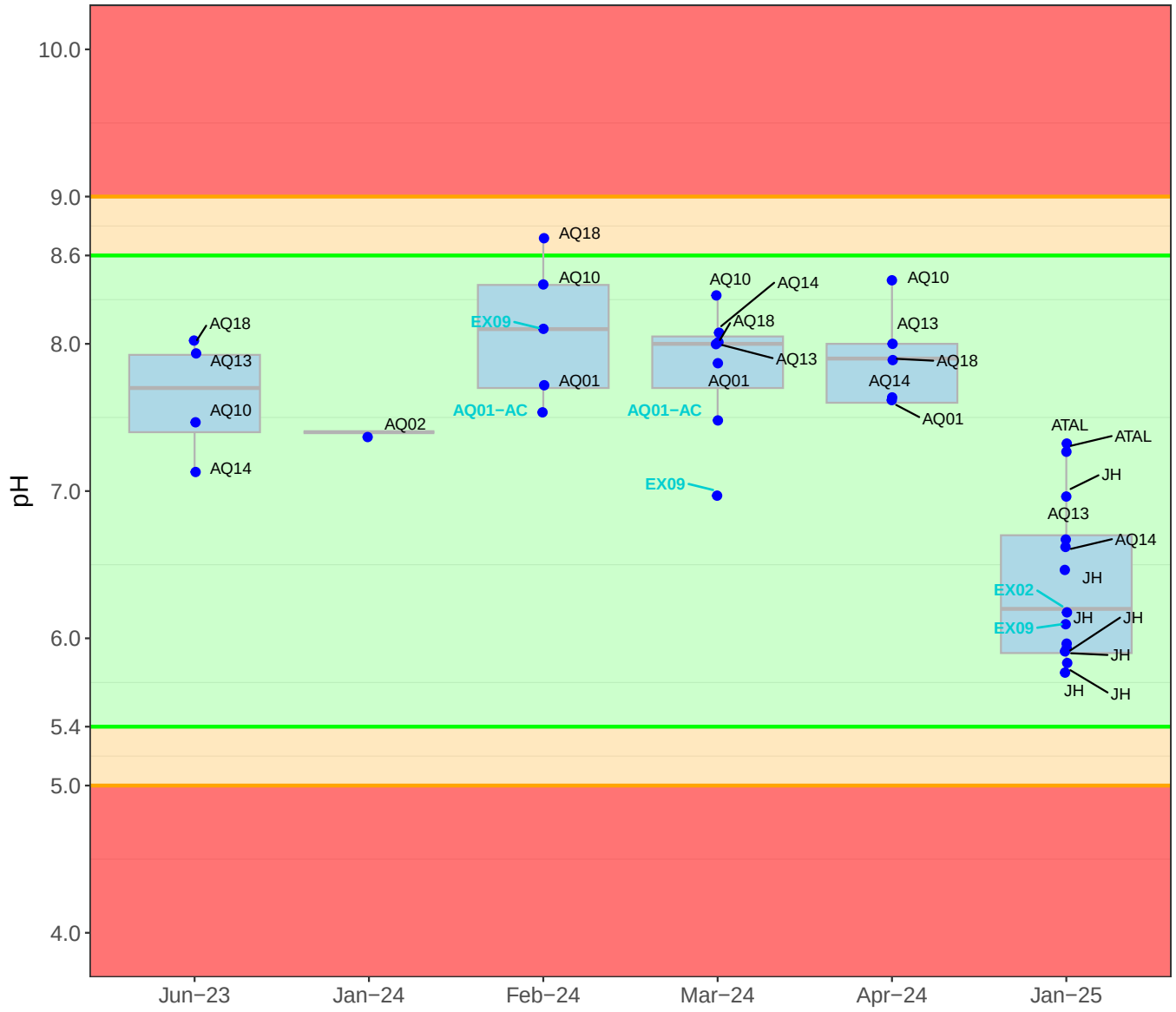

Figure A-1-1: Application of pH EQC to MRAMP rainfall measurements. The guideline EQC range is shown in orange, and the standard in red. EX09, EX02, and AQ01-AC (in aqua colour) are measurements from air conditioner condensate drain samples from the powered AQMs.

Figure A-1-1 shows the application of the *pH* EQC to MRAMP rainfall measurements. One measurement at AQ18 falls within the alkaline guideline EQC exceedance range. There is no known anthropogenic cause of alkaline readings on this outer island site. It is likely due to a combination of sea spray and alkaline minerals from surrounding limestone-rich islands. However, this will be further studied.

Figures A-1-2 and A-1-3 show the AS3580.10 total flask deposition data by month and by site

respectively. *pH* EQC are superimposed. Four alkaline values in the guideline and at the border of the standard region can be observed, however again these are at AQ18 (Collier Rocks) and AQ16 (Dolphin Island) and are most likely due to natural phenomenon. One value in the acidic guideline region at AQ08 (Burrup Peninsula) is evident which may be attributable to anthropogenic causes or may be due to guano deposition. Note that under the EQC criteria, *pH* values at AQ18 would only count as an exceedance if they occur in two successive months. Thus, Figures A-1-2 depicts one guideline EQC exceedance at AQ18 (August + September 2024 , upper *pH* limit).

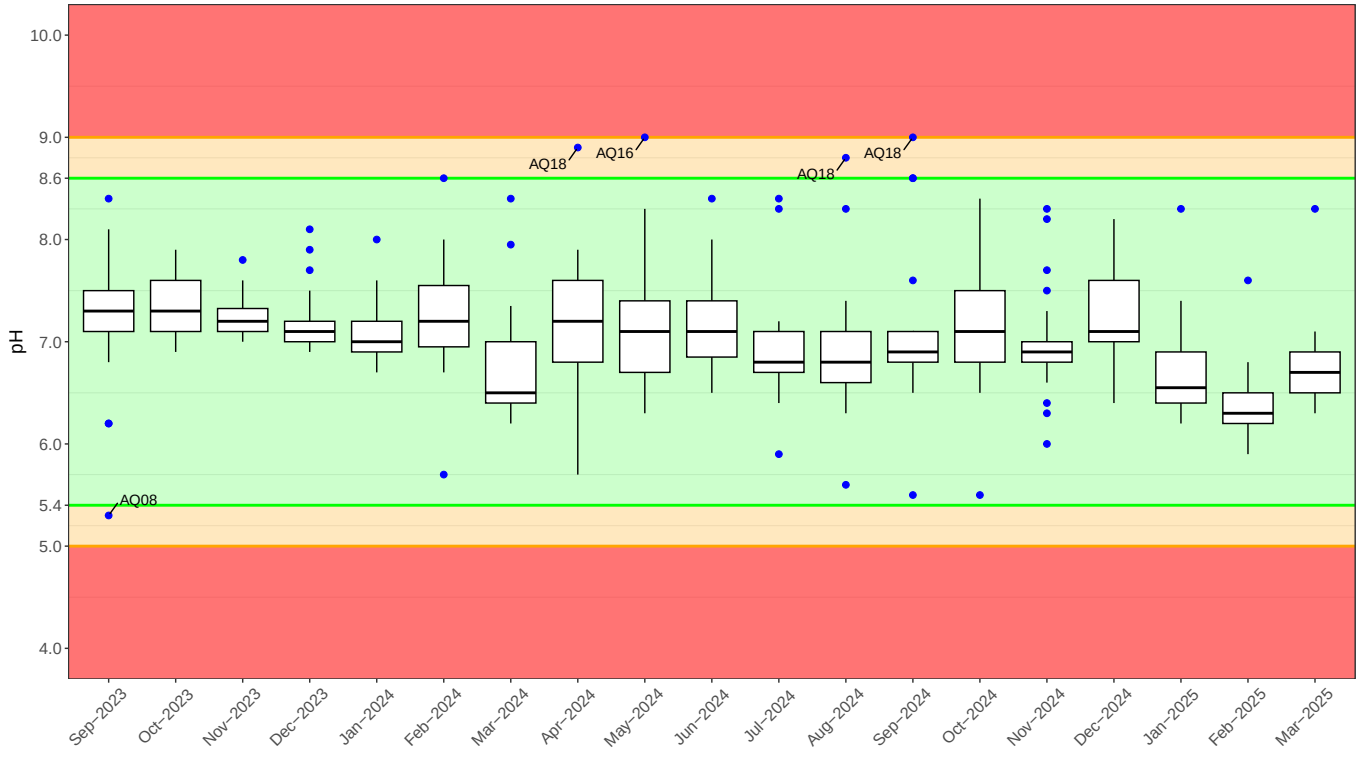

Figure A-1-2: Application of pH EQC to MRAMP total flask deposition (AS3580.10) measurements, plotted by month. The guideline EQC range is shown in orange, and the standard in red.

Figures A-1-4 and A-1-5 show the combined wet and dry bucket deposition data plotted by month and by site respectively. *pH* EQC are superimposed. A number of values in both the high and low *pH* regions are evident:

- EX02 shows a guideline exceedance in the alkaline (high *pH*) region (June + July 2024).
- AQ13 shows two periods (April + May 2024 and August-October 2024) which would constitute an exceedance of the low *pH* guideline.
- AQ08 shows an exceedance of the low *pH* standard (April + May 2024).

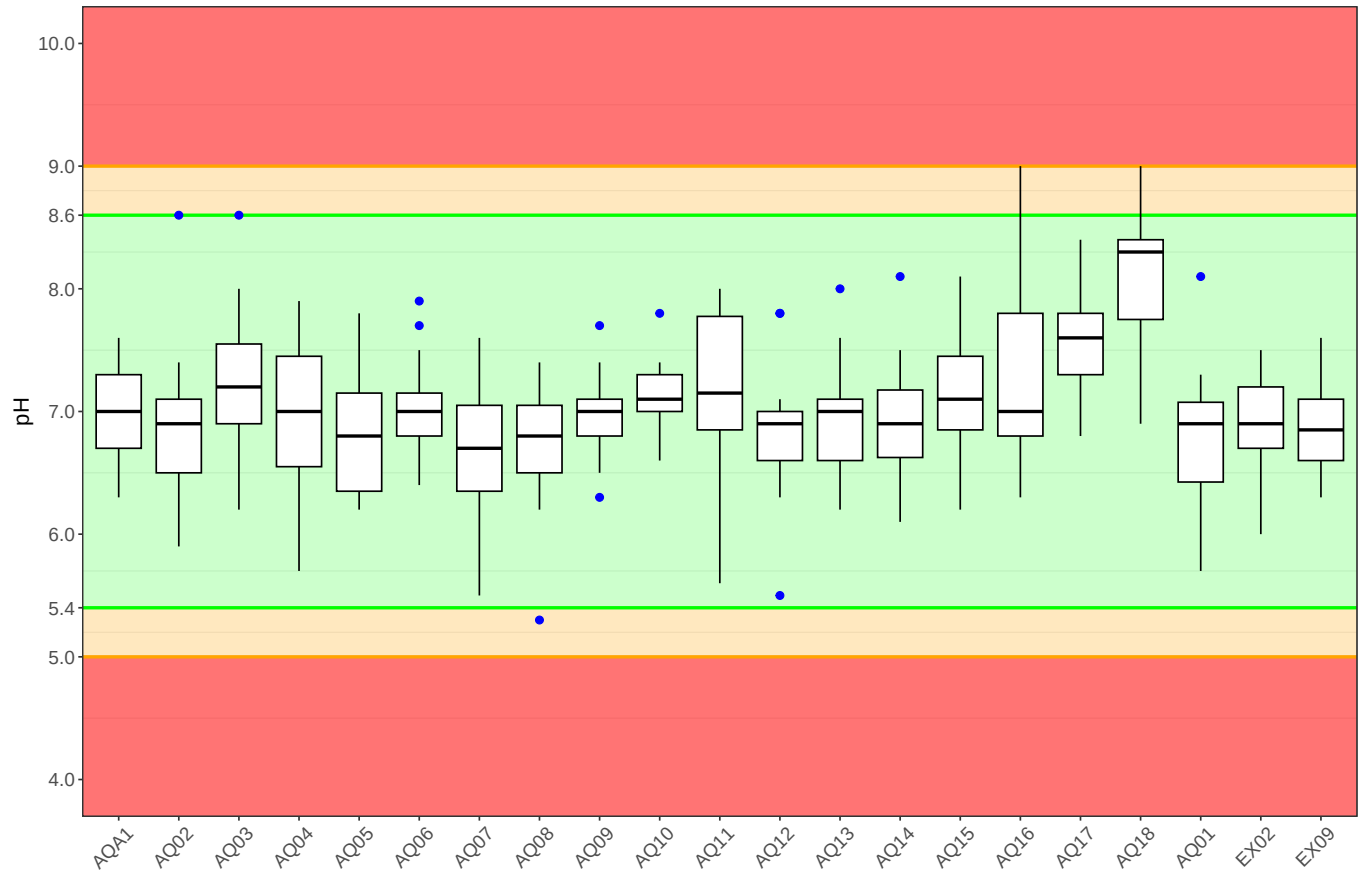

Figure A-1-3: Application of pH EQC to MRAMP total flask deposition (AS3580.10) measurements, plotted by AQM site. The guideline EQC range is shown in orange, and the standard in red.

Many of these high and low outliers do not correspond with total flask or IVL data and may be due to random contamination of the samplers with natural deposits. The cause of the high *pH* values at EX02 is not known and will be further investigated should they reoccur, as well as analysis of co-analytes. For the low readings, a possible explanation in some cases may be contamination of the samplers at AQM cages fabricated from weathering (Cor-Ten) steel with rust particles or flakes which may detach under high wind conditions and deposit in the samplers. This has been observed in some cases and would be expected to lower *pH*. This could explain the values at AQ13. These samplers are spread over the peninsula and archipelago as they were specified for any site close to rock outcrops to visually blend in with the surrounding environment. Figure A-1-6 shows the same dataset with bare weathering steel AQMs removed. This analysis excludes one third of the low pH outliers.

The low values in AQ08 cannot be readily explained as the AQM is not weathering steel. However the values do not closely correlate with total flask values or values at the co-located AQ07 station. A possible explanation is proximity to the Karratha Airport and the high level of sulfur which remain in most aviation fuels.

Based on the above considerations, the 3-bucket data should be treated with more caution at this stage while further cross-comparison with the total flask method is undertaken.

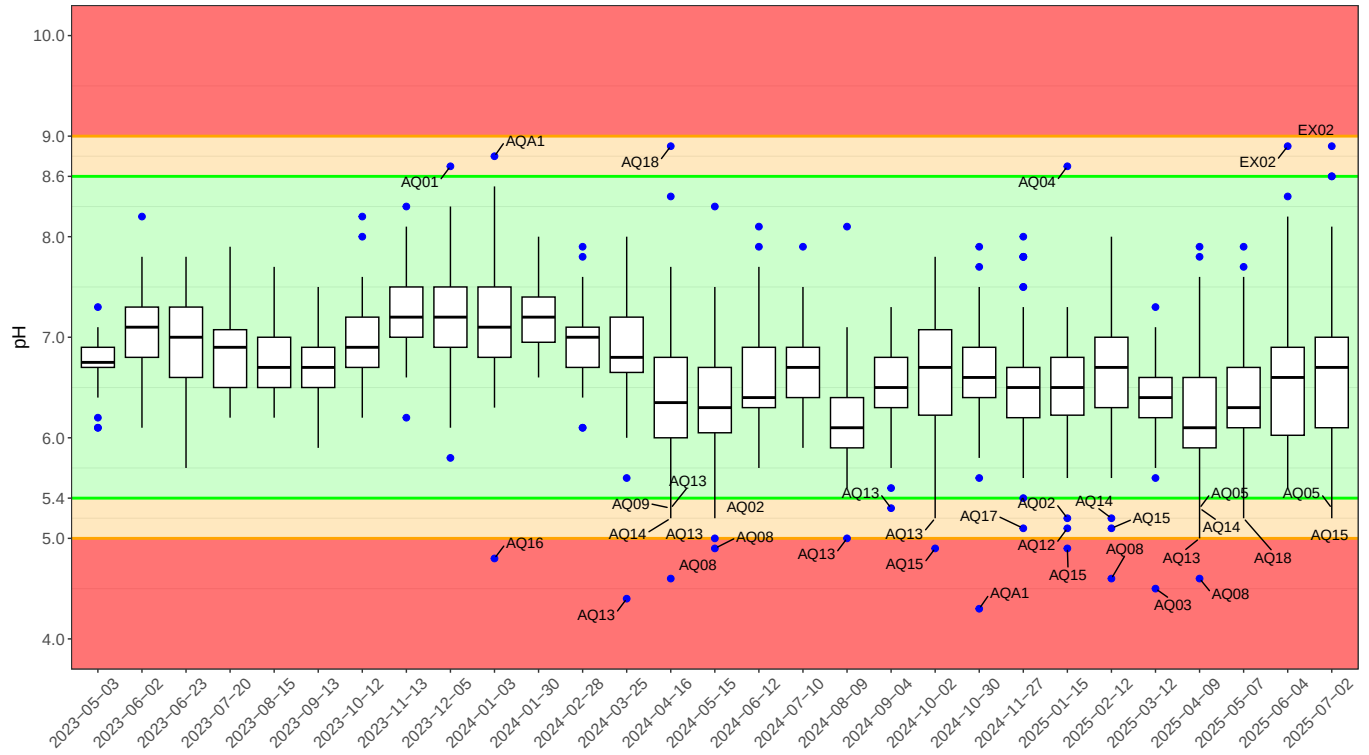

Figure A-1-4: Application of pH EQC to combined wet and dry deposition data from the novel three-bucket samplers, plotted by month. The guideline EQC range is shown in orange, and the standard in red.

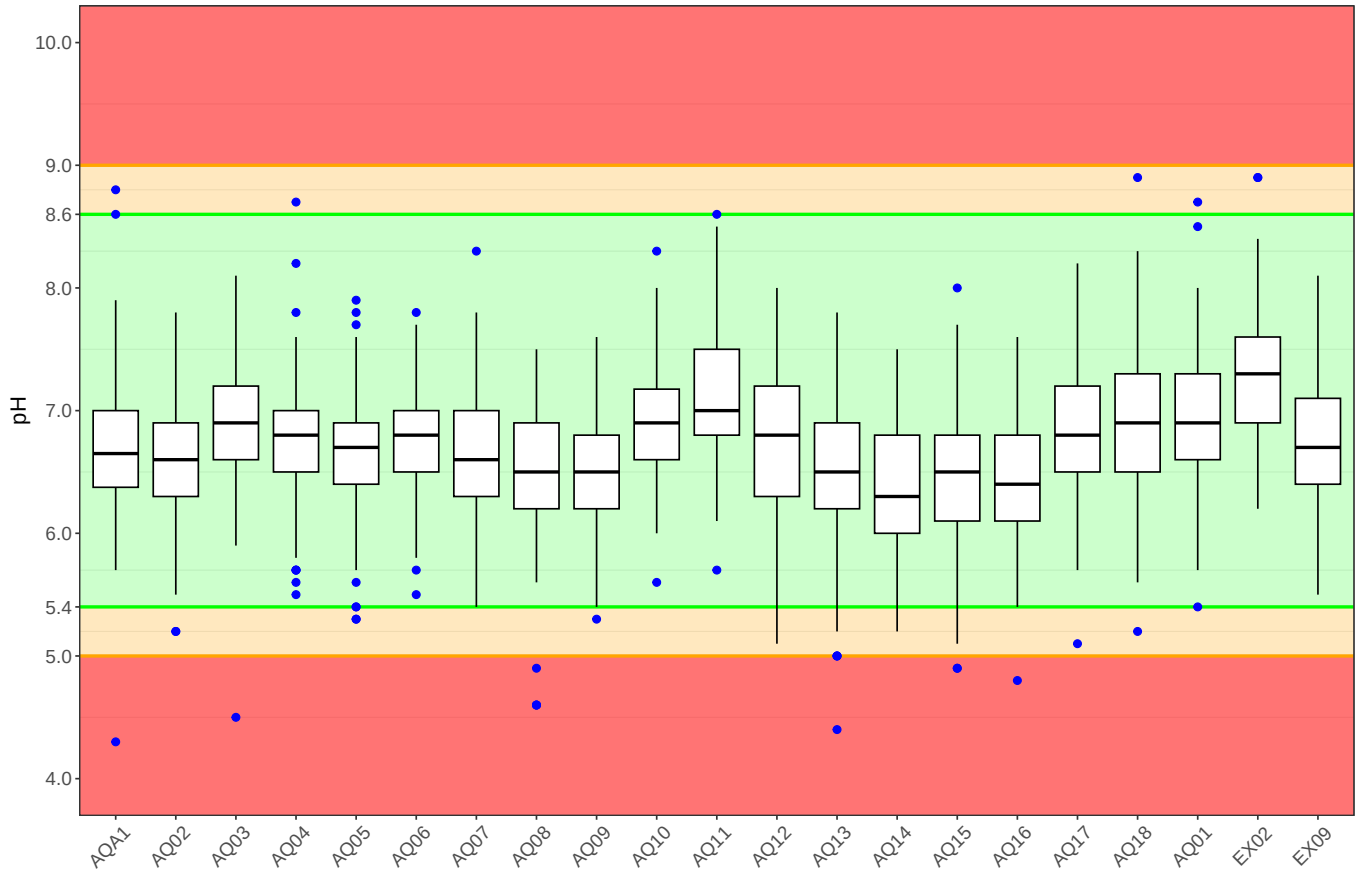

Figure A-1-5: Application of pH EQC to combined wet and dry deposition data from the novel three-bucket samplers, plotted by AQM site. The guideline EQC range is shown in orange, and the standard in red.

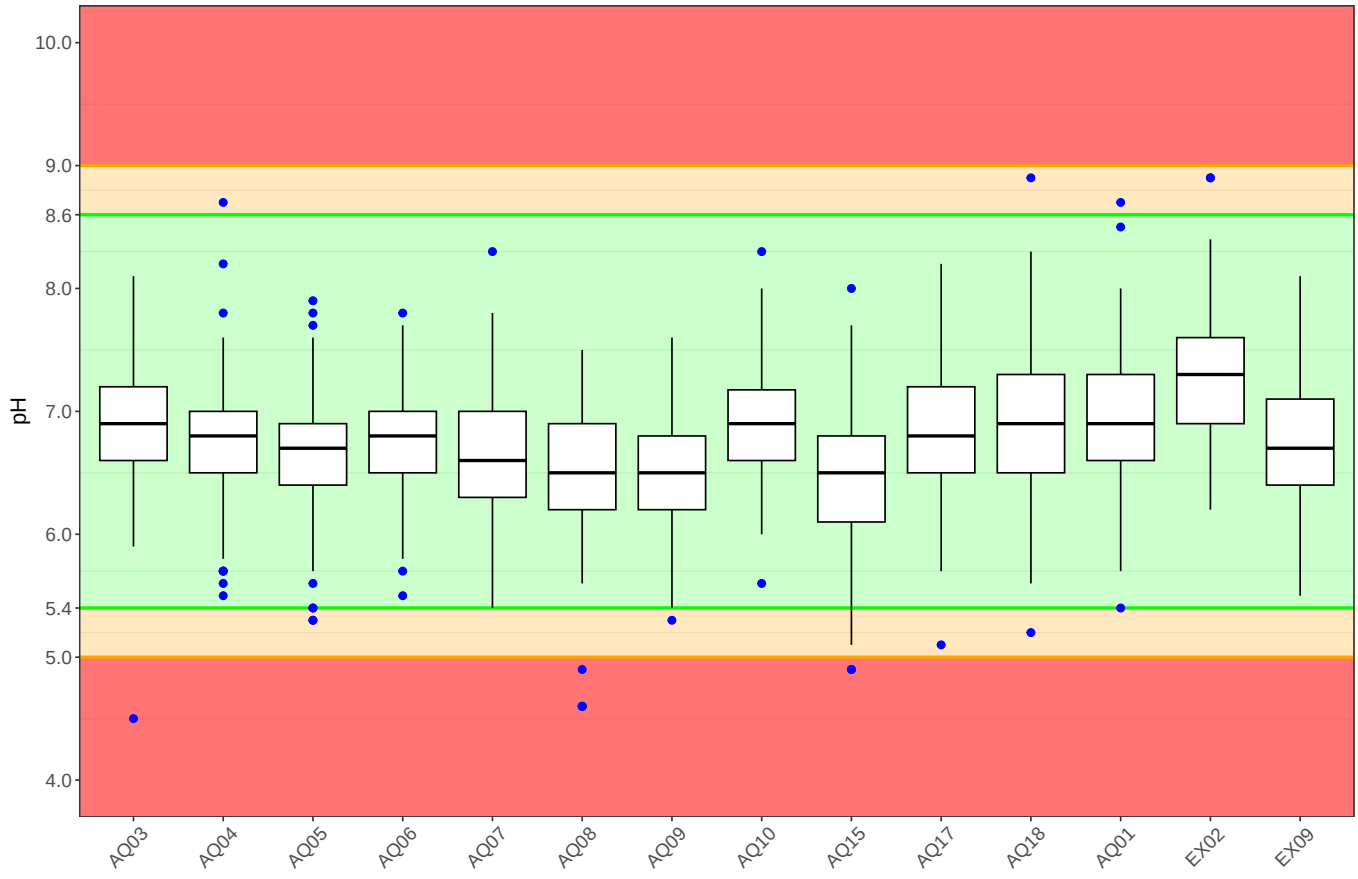

Figure A-1-6: Application of pH EQC to combined wet and dry deposition data from the novel three-bucket samplers, plotted by AQM site with weathering steel AQMs excluded. The guideline EQC range is shown in orange, and the standard in red.

A-2 Application of new air quality EQC to existing data from MRAMP passive samplers and powered gas analysers

A-2.1 Passive sampler data

It is expected that individual gas species EQC will be replaced by the weatherability index concept, however for the sake of completeness, MRAMP air quality measurements are presented here and compared to current Interim EQC and (where available) WHO human health guidelines.

Figures A-2-1 shows the last 2 years of IVL passive sampler measurements compared to the Interim guideline EQC (annual average). Figures A-2-1(a) also shows the WHO annual guideline for NO_2 for comparison. Note that the WHO annual guideline for SO_2 has been deleted and one for NH_3 has never existed.

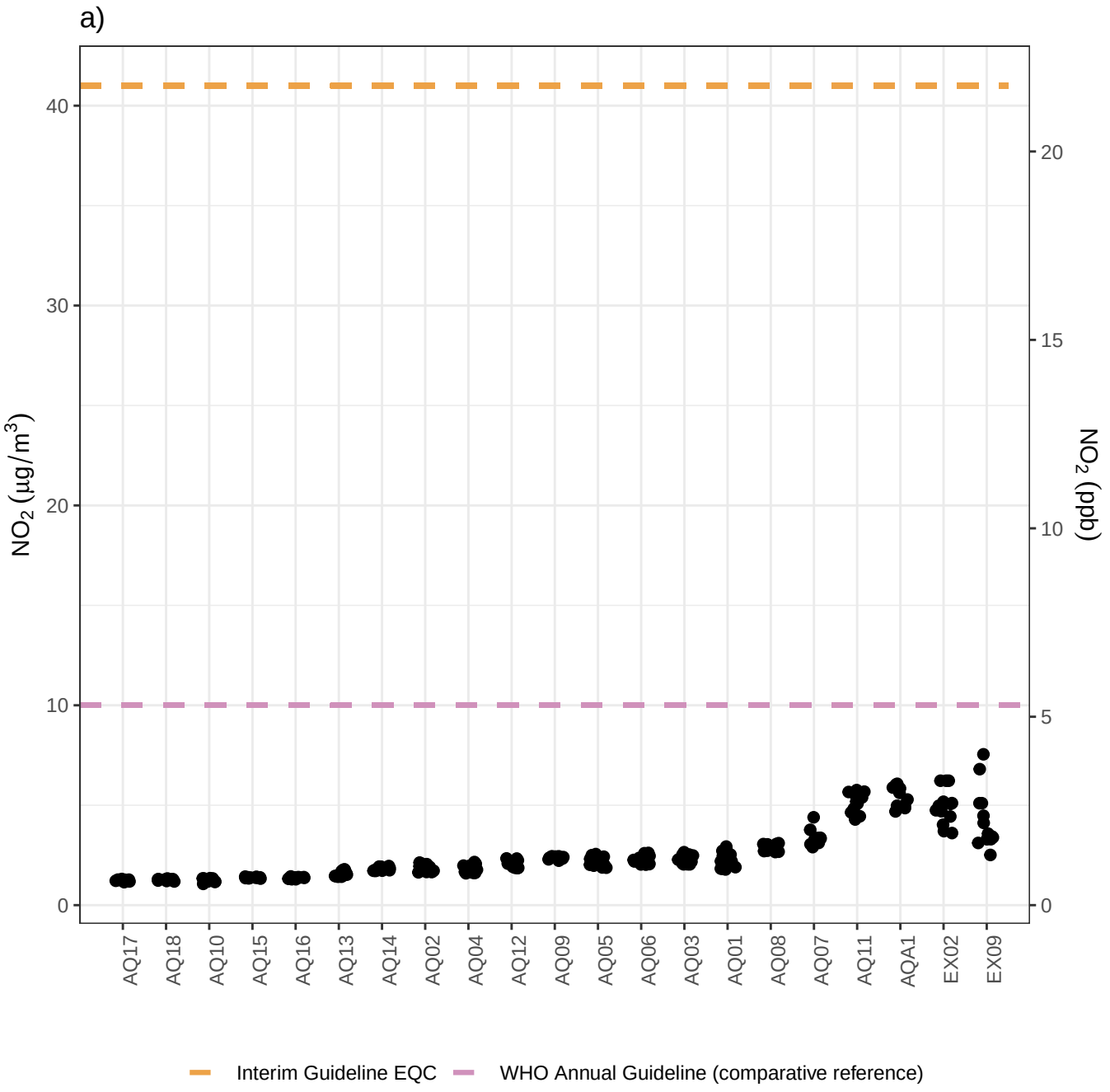

Figure A-2-1: Interim EQC (dashed line) and observed passive sampler average levels (●) at each MRAMP monitoring station (Nov 2022-Dec 2024). In each plot, sites are ordered by their overall average concentration of NO_2. To make the individual points ● more distinguishable, a small random offset (jitter) has been applied along the x-axis. Panel (a) NO_2.

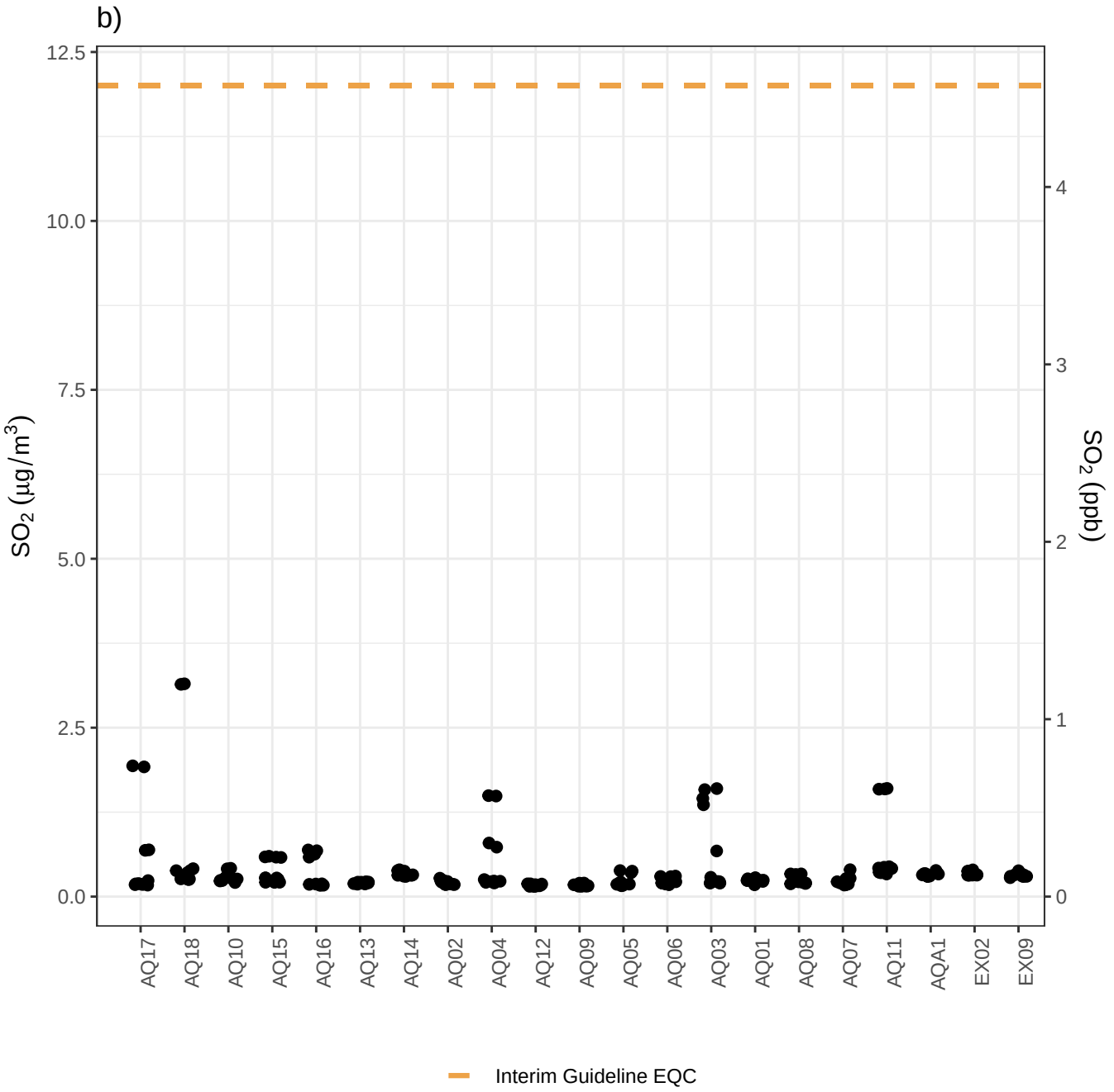

Figure A-2-1b) SO_2 (Continued caption from Figure A-2-1(a).)

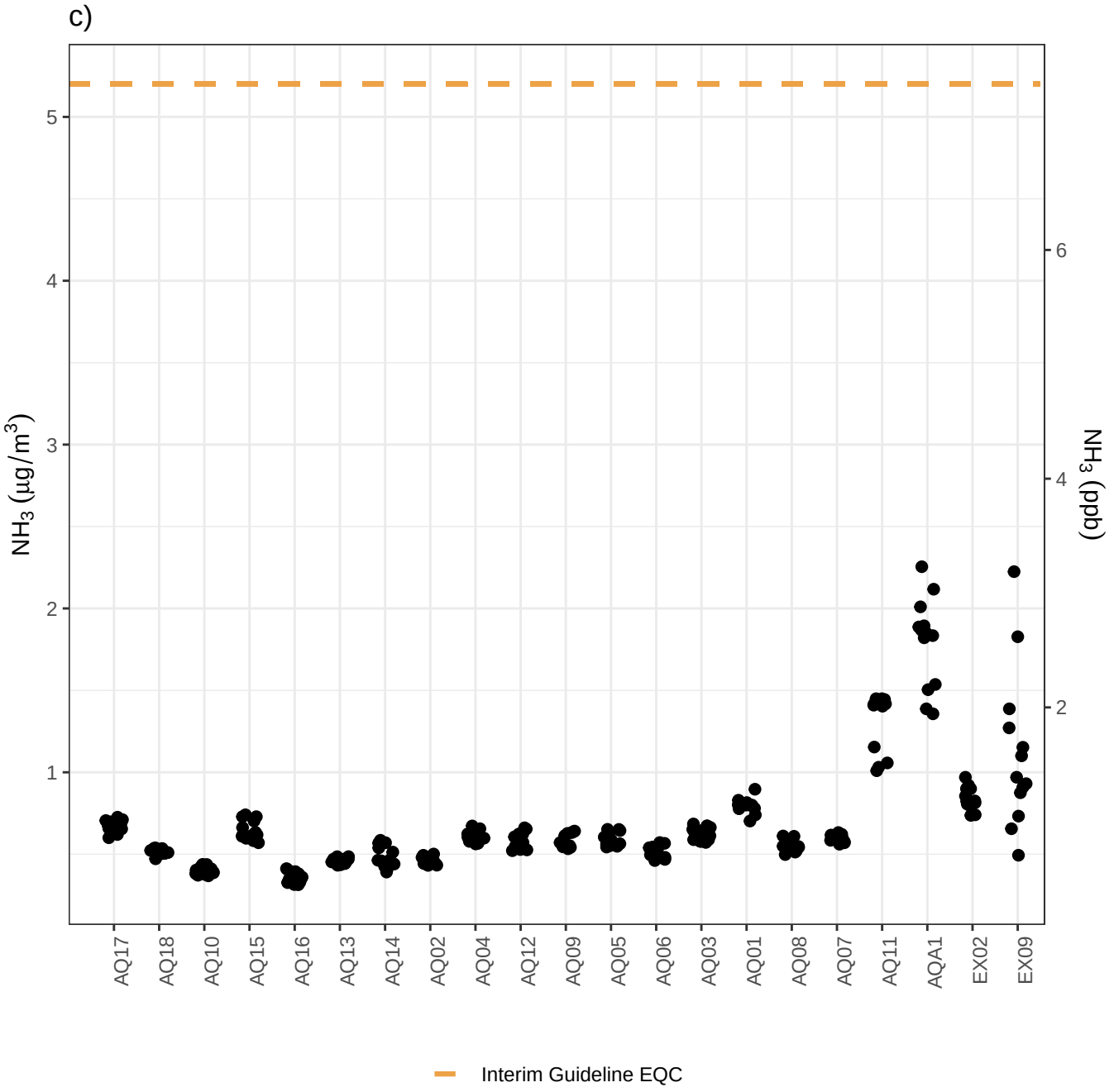

Figure A-2-1c) NH_3 (Continued caption from Figure A-2-1(a).)

A-2.2 Powered and passive sampler data

Figure A-2-2 shows MRAMP standard EQC (24 hour average) and WHO 24 hour average (human health) guidelines for NO_2. IVL passive sampler data for the three MRAMP operated powered AQM sites (AQ01, EX02, EX09) are also shown. Note that EX07 is operated by ACOEM for industry with additional equipment purchased and specified by MRAMP, and this AQM does not contain IVL passive samplers. As the MRAMP standard is now much higher than the previous standard (Curtin University, 2024a), Figure A-2-3 shows only the lower section of the y-axis. In this figure, one point that exceed the WHO guideline over the 13 months of MRAMP air quality measurements can be seen. No exceedances of the MRAMP EQC standards or guidelines were observed.

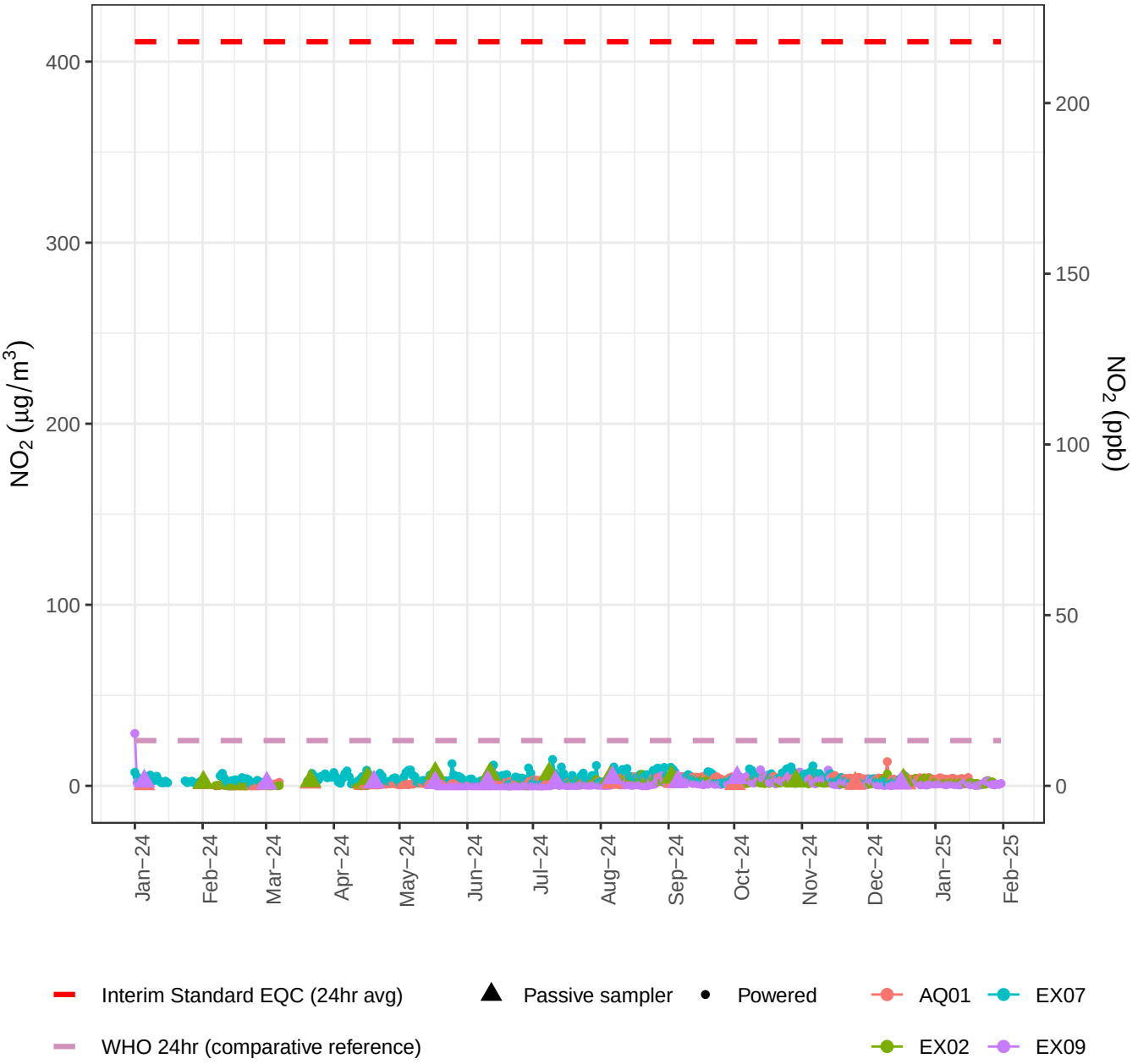

Figure A-2-2: Time series plots for NO_2 from January 2024 to February 2025 for the four powered air quality monitoring sites in the MRAMP network. The dots (●) are the daily mean NO_2 concentrations measured from the powered instruments. The triangles (▲) show the monthly mean NO_2 concentrations measured from the passive samplers. The red dashed line is the Interim Standard ECQ (24 hour average) and the mauve dashed line is the WHO 24 hour average exposure guideline for human health.

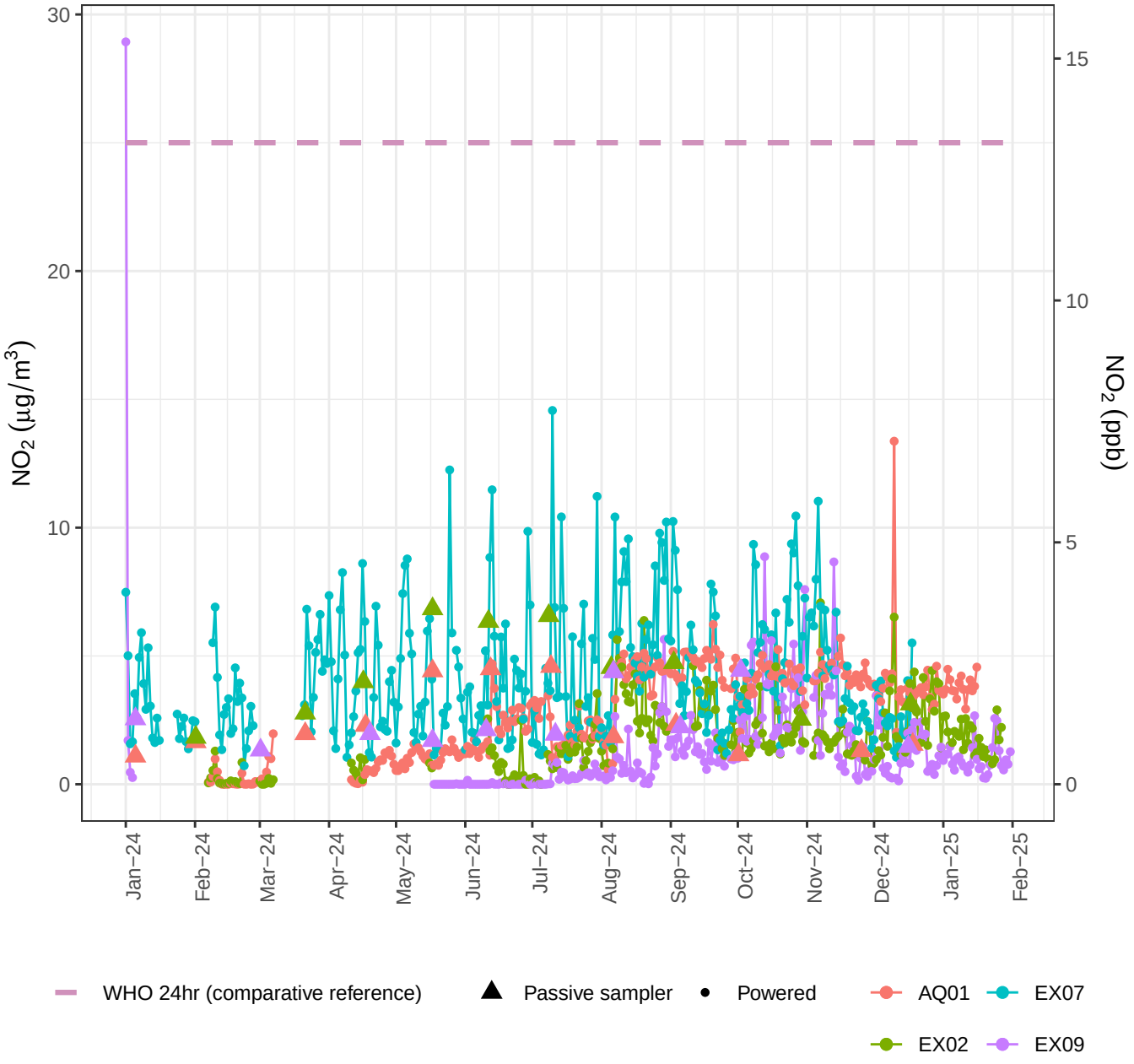

Figure A-2-3: Same as Figure A-2-2, but with the y-axis only between zero to 30 $\mu g/m^3$.

Figure A-2-4 shows the MRAMP standard EQC (24 hour average) and WHO 24 hour average (human health) guidelines for SO_2. IVL passive sampler data for the three MRAMP operated powered AQM sites (AQ01, EX02, EX09) are also shown.

Figure A-2-5 shows 24 hour average NH_3 data from the powered gas analysers. IVL passive sampler data for the three MRAMP operated powered AQM sites (AQ01, EX02, EX09) are also shown. An Interim standard EQC for NH_3 is not yet available. Note that the elevated NH_3 readings at EX02 between August-November 2024 are included in this figure as there was no known instrument error. However, as they do not correspond to elevated IVL passive sampler readings at the same time and location, the powered analyser readings are thought to be erroneous. The cause of the single peak at EX09 is not known but believed to be valid.

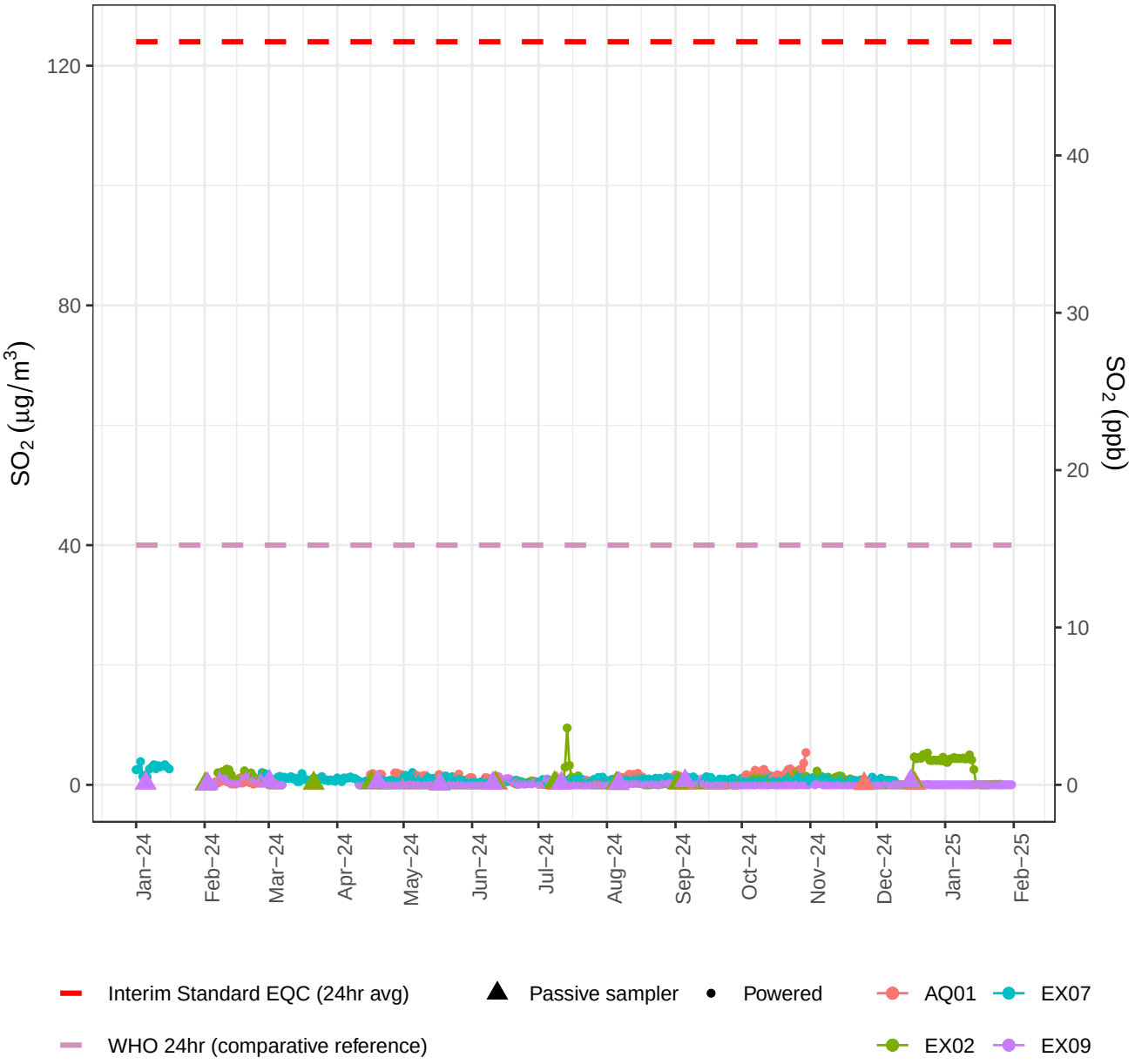

Figure A-2-4: Time series plots for SO_2 from January 2024 to February 2025 for the four powered air quality monitoring sites in the MRAMP network. The dots (●) are the daily mean SO_2 concentrations measured from the powered instruments. The triangles (▲) show the monthly mean SO_2 concentrations measured from the passive samplers. The red dashed line is the Interim Standard ECQ (24 hour average) and the mauve dashed line is the WHO 24 hour average exposure guideline for human health.

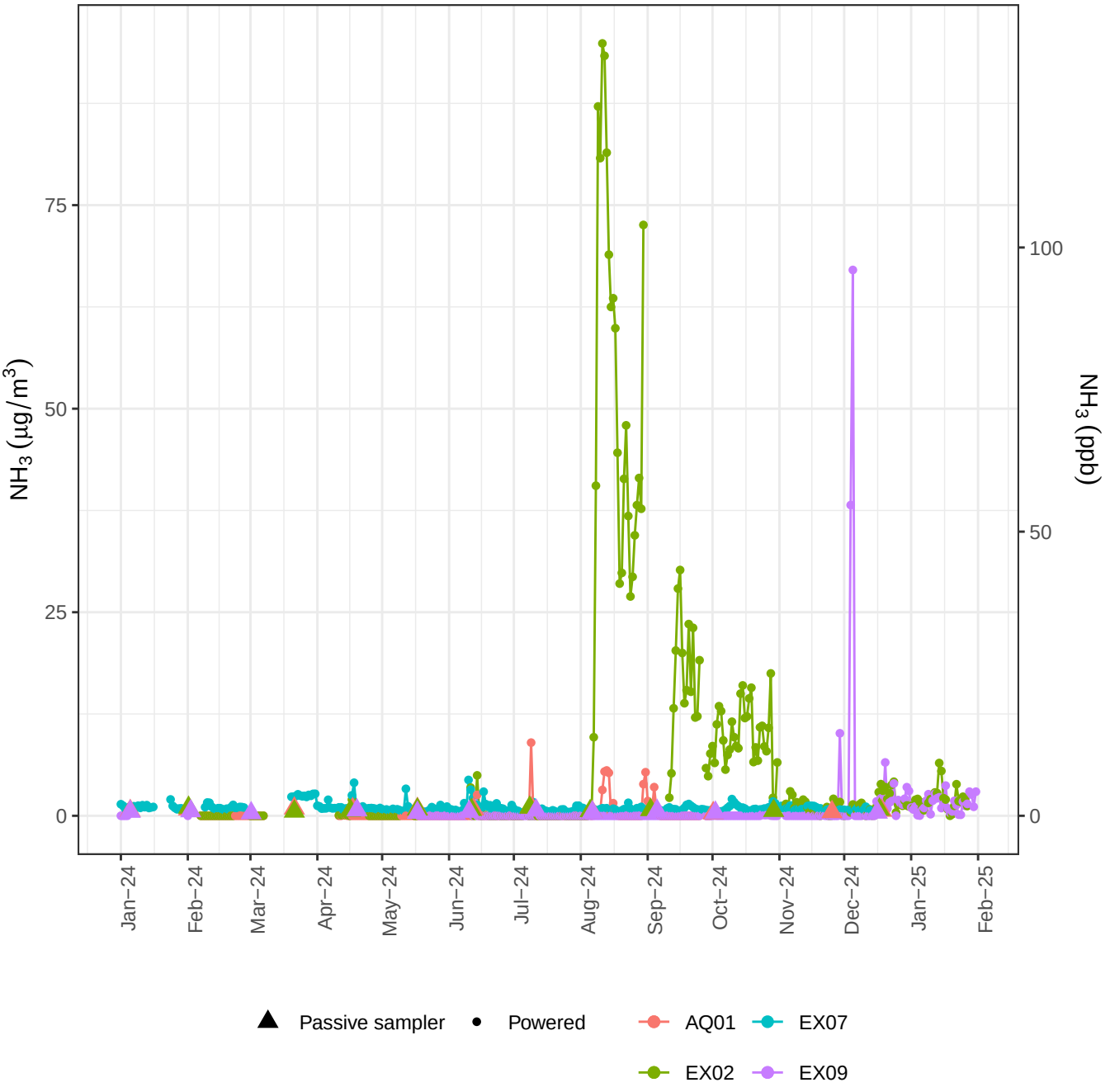

Figure A-2-5: Time series plots for NH_3 from January 2024 to February 2025 for the four powered air quality monitoring sites in the MRAMP network. The dots (●) are the daily mean NH_3 concentrations measured from the powered instruments. The triangles (▲) show the monthly mean NH_3 concentrations measured from the passive samplers.